Asteroseismic Analysis of Three SB_1 Systems using Photometric and Spectroscopic Observations

Georgia Rose

BSc Astrophysics and Chemistry (Honours)

Master of Science by Research

University of York

Physics, Engineering, and Technology

September 2024

Abstract

Pulsation frequencies were identified for three SB_1 binary star systems, two of which were confirmed γ Dor pulsators and the other being an elliptical variable, from both photometric observations, from the TESS mission, and spectroscopic observations, from the University of Canterbury Mt John Observatory (UCMJO) in New Zealand, of the target stars. For HD 217792 pulsation frequencies of: 0.670(2), 1.025(1), 1.278(2), 1.3813(7), 1.639(2), and 1.840(3) d^{-1} were determined from photometric observations and 0.661(1), 1.018(1), 1.278(2), 1.373(1), 1.625(2) and 1.838(2)d^{-1} were determined from spectroscopic observations. For HD 17310 pulsation frequencies of: 0.403(4), 0.453(6), and 0.558(3) d^{-1} were determined from photometric observations and 0.404(1), 0.455(1) and 0.544(8) d^{-1} were determined from spectroscopic observations. For HD 85964, an elliptical variable, frequencies of: 0.8008(1), 1.60200(2), 2.4029(2), and 3.2036(4) d^{-1} were determined from photometric observation and 0.8008(1), 1.6081(1), 2.4041(1) and 3.2089(2) d^{-1} were determined from spectroscopic observations. The results obtained from analysis of both sets of observations agree for most results to one or two decimal places but not within the errors of the results obtained from the photometric observations. These discrepancies in the determined frequencies could be attributed to the procedure used to determine the binary orbital parameters not accounting for any variations in radial velocity arising due to anything other than binary motion. This has been identified as the greatest contributing factor to the discrepancies identified between the two sets of results.

Acknowledgements

Many thanks to my supervisor Dr Emily Brunsden, without her guidance I would not have been able to achieve what I have, you have been invaluable.

To my family, partner and friends, thank you for reminding me that I am capable of more than I realise and for supporting me throughout.

This work made use of Lightkurve in the analysis of TESS light curves. (Lightkurve Collaboration 2018)

Author’s Declaration

I declare that this thesis is a presentation of original work and has not been presented for a degree or qualification from this university or elsewhere. I am the sole author of this work. All sources have been acknowledged as references.

Table of Contents

Abstract **1**

Acknowledgements **2**

Author's Declaration **3**

1. Introduction **6**

1.1 Types of Binary Star Systems **6**
1.1.1 Eclipsing Binaries 7
Figure 1.1 7
Figure 1.2 8
1.1.2 Spectroscopic Binaries 9
Figure 1.3 9
Equation (1.1) 9

1.2 Variable Stars **10**
1.2.1 Classification of Variable Stars 10
Figure 1.4 11
Figure 1.5 12
1.2.2 γ Doradus Variables 12
1.2.3 Mechanisms of Stellar Pulsation 12

1.3 Asteroseismology **13**

1.4 Selected Stars **14**
1.4.1 π PsA (HD 217792) 14
Figure 1.6 15
1.4.2 HD 17310 15
Figure 1.7 16
1.5.3 HD 85964 16
Figure 1.8 17

1.5 Observational Techniques **17**
1.5.1 Photometry using TESS 18
Figure 1.9 18
1.5.2 Spectroscopic analysis 18
Figure 1.10 19

1.6 Aims of Research **19**

2. Methodology ***20***

2.1 Photometric Analysis **20**

2.2 Spectroscopic Analysis **21**

2.3 Determining the reliability of Results **22**

3. Results and Discussion ***23***

3.1 π PsA (HD 217792) **23**
3.1.1 Photometric Analysis 23
Table 3.1 23
3.1.2 Spectroscopic Analysis 24
Figure 3.1 24
Figure 3.2 25
Figure 3.3 26
Figure 3.4 27
Table 3.2 27

Table 3.3 28
3.1.3 Comparison of Results 28
Table 3.4 28

3.2 HD 17310..29
3.2.1 Photometric Analysis..29
Table 3.5 29
3.2.2 Spectroscopic Analysis 30
Figure 3.5 30
Figure 3.6 31
Figure 3.7 32
Table 3.6 32
Table 3.7 33
3.2.3 Comparison of Results 33
Table 3.8 33

3.3 HD 85964..34
3.3.1 Photometric Analysis..34
Table 3.9 34
Figure 3.8 35
3.3.2 Spectroscopic Analysis 35
Figure 3.9 36
Figure 3.10 37
Figure 3.11 38
Table 3.10 38
Table 3.11 39
3.3.3 Comparison of Results 39
Table 3.12 39

3.4 Comparison of Results for All Stars 40

4. Conclusion.. 41

References 42

1. Introduction

The study of the stars is an ancient pursuit, one spanning many millennia. It began with simply charting the stars and tracking their movements through our skies; in more recent history it has advanced to a more detailed study of the stars themselves. Our measurements of the position and movements of them is much more precise with the advancement from ground-based to space-based telescopes. This has also allowed for detailed analysis of the light emitted from the star and allowed for determination of variation in brightness, colour temperature and, whether a star exists as part of a multiple system.

The study of binary star systems, two stars orbiting each other about their centre of mass, has enabled astrophysicists to calculate a star's mass independent of its distance from the observer as well as understand the limb-darkening, the gradual tapering of opacity at the star's edge. Dependent upon the angle at which a binary star system is observed it can appear to be variable relative to the observer; this is due to the star's motions about each other, as detailed below.

Asteroseismology is a field that is concerned with the study of stellar pulsations and the driving forces behind them. Through these studies we can probe the interior of stars and gain greater insight to their structure; with different types of pulsators occupying different regions of the Hertzsprung-Russel diagram. We can see how stellar structure varies based on factors such as, their mass, temperature and evolutionary phase [1]. Many asteroseismic studies to date have focused on single pulsating stars, as these are the most straight forward, developing techniques for using both photometric and spectroscopic data. In this study I will combine the study of binary stars and asteroseismology by undertaking asteroseismic analysis of single-lined spectroscopic binary star systems, binary star systems for which only the primary star can be spectroscopically observed due to the secondary being too faint for observation. Bringing together these two fields of research affords researchers the opportunity to observe how pulsations can appear differently, dependent upon whether the star is a single star or exists as part of a binary star system, and how once the binary effects are removed a candidate pulsator may not be pulsating. It also makes possible the determination of a stars mass independent of the asteroseismic results.

1.1 Types of Binary Star Systems

The different types of binary star systems are categorised by the way in which we can observe the effects of the binarity; whether we can directly observe the motion of the two stars or, see the effect the secondary star is having on the primary without being able to image the secondary directly. The study of binary star systems extends beyond the determination of orbital parameters. It is possible from observations of these systems to determine the masses and radii of the component stars. Data collected as part of the Wide Angle Search for Planets (WASP) survey has been utilised by the EBLM

Project paper 4 [2] in order to determine the mass and radius of the component stars in low-mass eclipsing binary systems. This work is being undertaken by the collaboration with the aim of reducing the inconsistencies between observations and stellar evolution models by taking more mass, radius and luminosity measurements of these stars. Discussed below are the two types of binary system that form part of this work and how both can be utilised to gain insight into different properties of the stars and their orbits.

1.1.1 Eclipsing Binaries

In 1782, the first eclipsing binary star system was discovered by Goodricke named Algol. Its discovery was due to periodic variations in the stars brightness as the two component stars orbit about their common centre of mass [3]. When i, the orbital inclination as illustrated below in Figure 1.1, is approximately 90° the two stars in the system can be seen passing in front of each other. This can be seen in Figure 1.2 below. The larger decrease in brightness is due to the smaller secondary star passing behind the larger primary star, referred to as an eclipse. The smaller decrease in the systems brightness is due to the secondary star passing in front of the primary star, referred to as a transit. This assumes that the orbit is circular and does not have any eccentricity, e, causing the orbit to take on a more oval shape due to the difference in masses of the two stars [4].

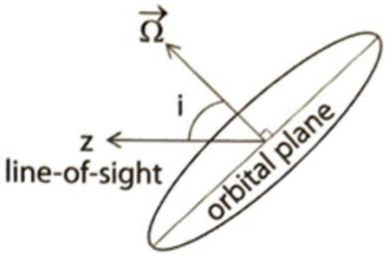

Figure 1.1: A schematic of a binary orbit, Z is the line of sight to an observer, i is the orbital inclination, 90° for an eclipsing binary system, Ω is the angular velocity. Image from [4].

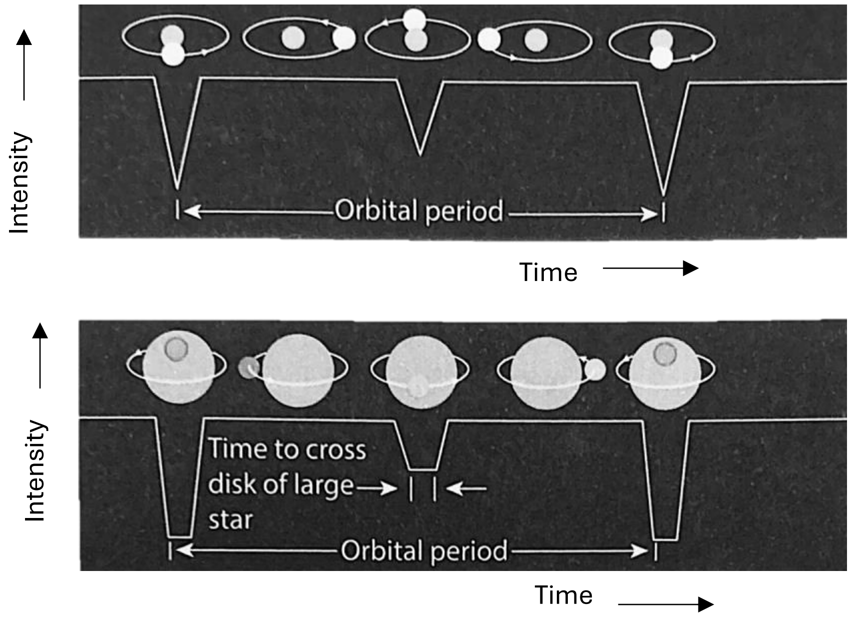

Figure 1.2: A schematic of a light curve for an eclipsing binary star system, top showing a partial eclipse and bottom showing a total eclipse. The larger decrease in brightness is due to the smaller secondary star passing behind the larger primary star, referred to as an eclipse. The smaller decrease in the systems brightness is due to the secondary star passing in front of the primary star, referred to as a transit. This is when observing Algol systems, it is reversed when observing EBLM systems. Image from [4].

Eclipsing binary star systems are the easiest to obtain orbital periods for, providing that they have been observed continuously for at least 1 orbital period and ideally over multiple orbital periods. As seen above in figure 1.2, the orbital period can be obtained from noting the time between eclipses. In the case of fully eclipsing systems, the shape of the trough in the lightcurve can also provide information on the limb darkening of the primary star; assuming the secondary star is significantly dimmer than the primary star. Mass, radius and effective temperature measurements can also be taken from the light curves of these systems, the methods for which are outlined in Swayne et al 2021 [5]. For example, the study of these systems has formed a series of papers titled The EBLM Project [6], focussing on low-mass eclipsing binaries, the first of which was published in 2013 and is an on-going research collaborative between many institutions across the globe.

1.1.2 Spectroscopic Binaries

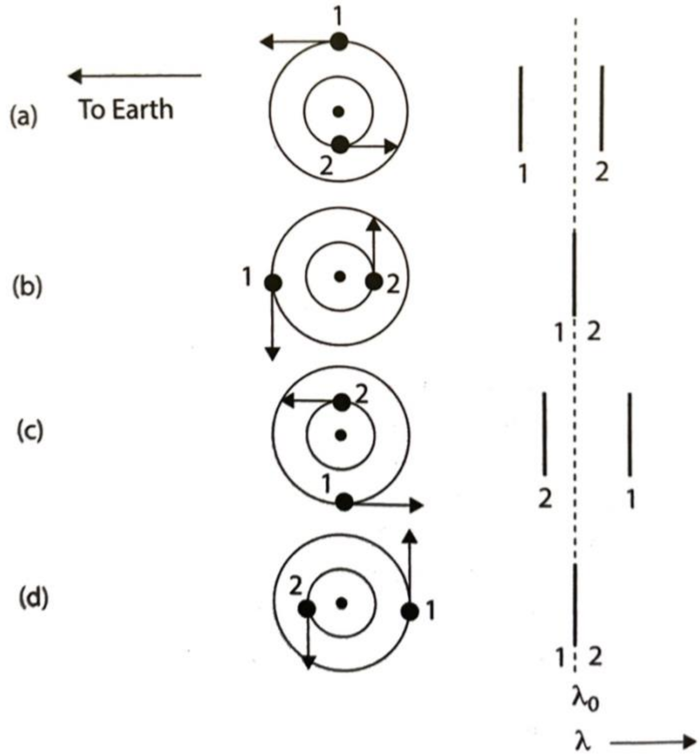

Figure 1.3: A schematic of how a binary star systems orbital motion causes a Doppler shift in the spectral lines in a system where the stars have approximately the same brightness, λ is the wavelength of the lines due to the Doppler shift and λ_0 is the wavelength when it is not shifted. Image from [4].

The first spectroscopic binary system was one of the components of Mizar, discovered in 1889 by E. C. Pickering [3]. Spectroscopic binaries, the focus of this research, are identified by a shift in the spectral lines of the star as it moves towards and away from the observer, as seen above in Figure 1.3. As star 1 moves towards the observer wavelength decreases and as it moves away from the observer wavelength increases; when the stars are moving perpendicular to the line of sight of the observer, no change in wavelength is observed. When the spectrum of both stars can be resolved, and a periodic doubling of the spectral lines is observed, the system is classified as a double-lined spectroscopic binary, SB2. When only the primary star is able to be resolved, due to the secondary star being too faint to be observed, the system is referred to as a single-lined spectroscopic binary, SB1. The formula for Doppler shift, equation 1.1 below, can be used to convert these changes in λ to radial velocity, v_{rad} [4]

$$\frac{\Delta\lambda}{\lambda} = \frac{v_{rad}}{c}$$

Equation (1.1)

By changing these spectroscopic observations from wavelength to radial velocity a Radial Velocity (RV) curve can then be produced, plotting time against radial velocity, which can then be fitted using a sinusoidal function to obtain the binary systems orbital parameters.

Spectroscopic binary systems are still being discovered, many of which are variable stars that have been previously discovered that can now be classified as spectroscopic binaries, due to advances in equipment and techniques. For example, Shetye et al 2024 [7] have now classified 32 Cepheid variables in the Milky Way galaxy as spectroscopic binaries; classifications that were made due to the utilisation of high-precision velocity measurements made as part of the VELOcities of CEpheids (VELOCE) project.

1.2 Variable Stars

Stars do not necessarily require a binary companion in order to exhibit periodic variations in their brightness, a single star can also display variability. The variable nature of single stars can be due to pulsations within the star causing it to periodically expand and contract. There are two common modes of pulsation in stars the latter of which will form the focus of this work: p-modes, where the resorting force is pressure and g-modes, where the restoring force is buoyancy. Both of these pulsation modes allow us to probe the interior of stars and “see” beneath their surface to better understand their structures [8]. The following sections discuss what makes stars appear variable, the driving mechanisms behind stellar pulsations and classifications of variable stars.

1.2.1 Classification of Variable Stars

Over longer time scales, hydrostatic equilibrium holds true for variable stars; over shorter time scales, there are different processes occurring in different parts of the star’s structure that lead to detectable pulsations. Stars do not all share the exact same structure, a star’s age, elemental composition, formation location and generation all have an effect on the internal structure. Stars that have fused elements of higher mass within the core have envelopes of these different atoms at different distances from the core. Main-sequence stars of lower mass have a large convection envelope for their outer layer, within the convection envelope heat energy is transferred to the stellar surface to be emitted radiatively [9]. These structural differences are what lead to each type of variable star displaying unique oscillations. The regions on the Hertzsprung-Russell, HR, diagram responsible for each type of variable star can be seen below in Figure 1.4. Each type exists in its own discrete region [8].

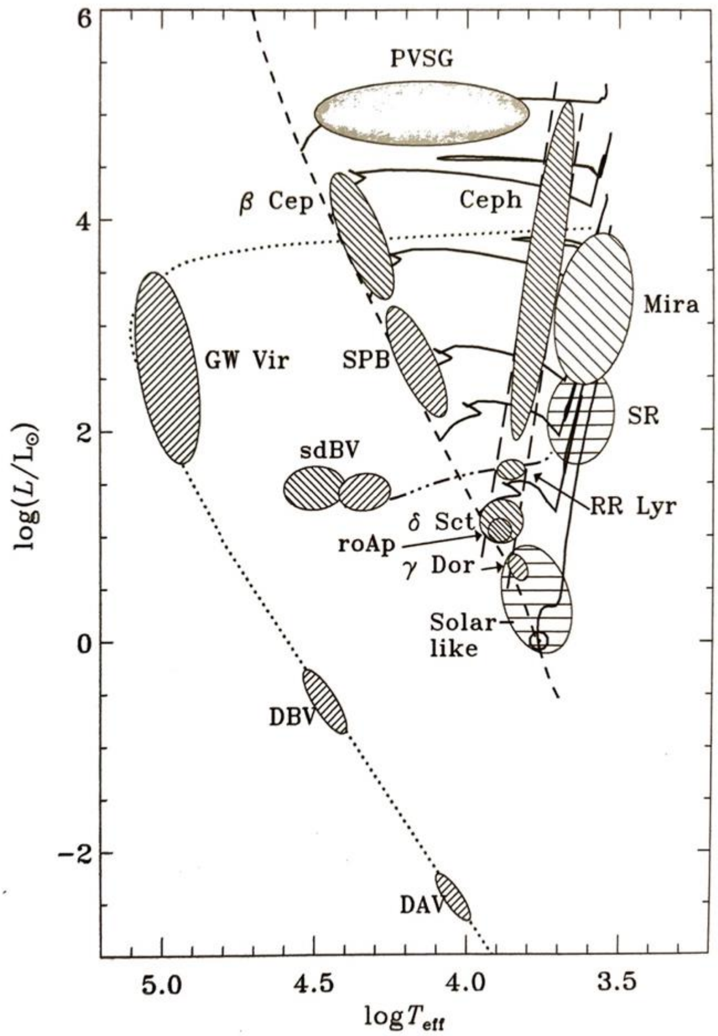

Figure 1.4: Hertzsprung-Russell Diagram illustrating the region occupied by different classes of pulsating stars, plotting $\log T_{eff}$ against $\log(L/L_{\odot})$. This highlights how stellar properties differ between different classes of pulsator. γ Doradus pulsators can be found in the upper region of the Solar-like pulsators, with $\log T_{eff}$ approximately 3.8 and $\log(L/L_{\odot})$ approximately 0.75. Image from [8].

δ Scuti and β Cephei stars have higher pulsation frequencies which are attributed to p-mode pulsations. These are confined to the outer layers of stars; this is due to changes in the density of the stellar matter as the pulsations attempt to travel towards the star's interior, because of the associated change in the speed of the sound. In contrast, g-mode pulsations are confined to the central regions of stars. Being trapped beneath the star's convective envelope, these pulsations are more sensitive to changes in conditions surrounding a star's core. G-mode pulsations are typically found within stars exhibiting oscillations at lower frequencies, for example γ Doradus pulsators [8]. Figure 1.5 below illustrates how each of the pulsation modes are confined to specific regions of the stellar interior; due to being confined to the core region of a star, g-mode pulsations are useful for gaining insight into the innermost structure and conditions present within a star.

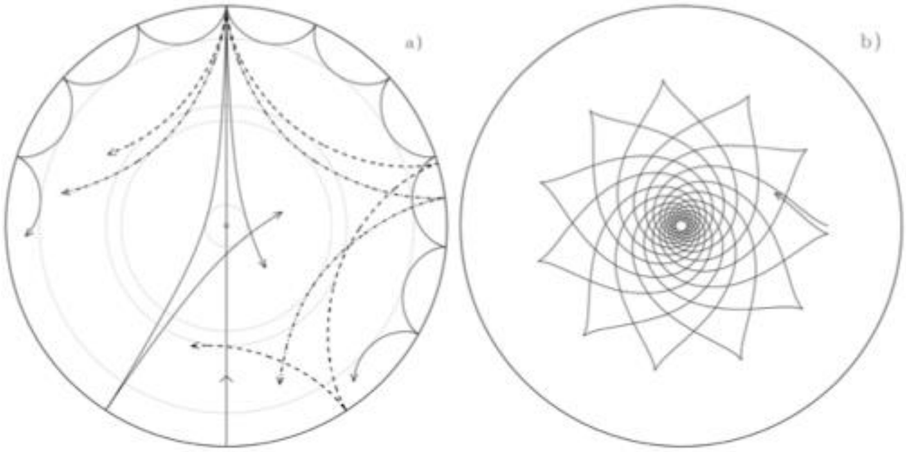

Figure 1.5: Ray path diagram of: a) p-mode pulsations and b) g-mode pulsations, both modelled at higher modes. P-mode pulsations are mostly contained to the outer layers of stars due to changes in the density of stellar matter towards the star's interior. G-mode pulsations are confined to the central region of a star and trapped beneath a star's convective envelope. Image from [8].

1.2.2 γ Doradus Variables

As shown on Figure 1.4 above, γ Doradus (γ Dor) pulsators occupy a relatively small region on the HR diagram, compared to other classifications of pulsator. This class of pulsators are named after the star γ Dor, the first of this type of pulsator identified by Cousins and Warren (1963) as well as being the most well studied star of this type. (L. Balona 1994) As stated in [11]. These stars are g-mode pulsators, typically with periods ranging from 8 to 80 hours, or in the frequency range of 0.3 to 3 d^{-1}. They lie on the red edge of the main-sequence instability strip on a HR diagram, they are late-A to early-F type stars [10] and their mass typically lies in the range of 1.3 to 2 $M_{\odot}$ [11]. γ Dor stars are the ideal pulsator to use for the study of convective core physics, due to their shallow convective envelope causing g-mode pulsations. As illustrated above in Figure 1.5, g-mode pulsations remain confined to the stars inner layers and can allow us to probe the interface between the stars radiative and convective layers. Due to the majority of γ Dor pulsators having frequencies at approximately 1 d^{-1} ground-based studies are difficult, but due to having multiple space-based observatories that have been operating for multiple years it is now possible to perform asteroseismic studies of these stars [11].

1.2.3 Mechanisms of Stellar Pulsation

These pulsation modes are driven by different oscillation mechanisms within stars. As stars expand and contract, they heat and cool. Typically, the radial layer of the star heats during the contraction phase of the pulsation and drives the stars cycle of pulsation. When this occurs successfully the star will function as a heat engine. Heat energy is converted to mechanical energy [8].

Within certain types of stars there are ionisation layers for hydrogen and helium, the high opacity of these layers can block radiation that is being emitted from the stars core. This leads to an increase in the temperature and pressure causing the star to expand beyond its equilibrium state. These temperature and pressure increases in turn lead to the H or He becoming ionised which, reduces the layer's opacity allowing radiation to pass through. The gas now cools and is no longer able to support the weight of the outer layers. This leads to a contraction. Once the star has contacted the H and He can recombine, opacity is now increased, and the cycle begins again. This is referred to as the κ-mechanism [8].

Throughout the majority of a star's life cycle, it is evolving over an extended period of time, existing in a state of near constant hydrostatic and thermodynamic equilibrium. This brings us back to the origin of p-modes and g-modes of oscillation; the internal pressure gradient of the star pushes outwards whilst the gravitational force is acting inwards. The restoring force in p-mode pulsations comes from fluctuations in the star's pressure gradient whereas, in g-mode pulsations the restoring force is due to the buoyancy of the gas within the gravitational field. For a star to remain in hydrostatic equilibrium both of these forces need to remain equal. When they are, the star is able to maintain a constant radius, not collapse under its own gravity and not expand beyond the point of being a single celestial body [12]. By understanding the mechanisms behind stellar pulsations, observations of pulsating stars can be taken and analysed, using methods outlined below, and utilised in order to advance understanding of stellar interiors.

1.3 Asteroseismology

A relatively new field within astronomy, asteroseismology is concerned with the study of stellar pulsations in order to probe a star's internal structure. As discussed above, pulsations travel from within the interiors of stars, confined to different regions and holding information on stellar structure. A field emerging in the early 1990's, it allows us to translate information from the star's surface to information about the star's interior structure. The frequency of pulsations that we observe at the stellar surface is dependent upon the time taken for the wave to travel along its ray path, therefore, it depends on the integral of the speed of the sound within the region it travels. If we are able to observe modes that are able to penetrate all different depths of the star's interior, it is then possible to use these observations to calculate the speed of sound throughout the star. By doing this, that star's temperature profile can be determined, using reasonable assumptions about its chemical composition based on known properties. Helioseismology has resulted in the speed of sound within the sun being known for over 90% of its radius [8]. This has resulted in the improvement of stellar models and advanced our understanding of stellar evolution. The aim of asteroseismology is to do this for many more stars.

1.4 Selected Stars for Asteroseismic Analysis

Three single-lined spectroscopic binary star systems are studied as part of this work, π PsA, HD 17310 and HD 85964, the first two being confirmed γ Dor pulsators and the third being a rejected candidate γ Dor. HD 85964 is being used for purposes of comparison within this work.

1.4.1 π PsA (HD 217792)

π PsA is a relatively well studied SB_1 [13] γ Dor pulsator with a spectral type F1V [14]. It has a low mass companion with an orbital period of 178d [15] [16]. Other properties of this binary system include: an eccentricity of 0.53 [17] as seen in [18] and a velocity amplitude of 21.3 km s^{-1} for the primary star [16]. Other known stellar parameters for this star found by David & Hillenbrand 2015 [19] are: T_{eff} (effective temperature) = 7400 $\pm$ 250 K, log g = 4.3 and $M_{\odot}$ (stellar mass) = 1.5 $M_{\odot}$; further known parameters include: ν_{turb} = 2 km s^{-1} [14], [Fe/H] (metallicity)= –0.25 $\pm$ 0.06 [20] as seen in [18] and R (radius) = 0.87 $R_{\odot}$ [21] as seen in [18].

A spectroscopic study of this system carried out by B. W. Bopp et al 1970 [22] in order to obtain its orbital elements found: γ (systemic velocity) = –5.97 $\pm$ 0.11 km s^{-1}, K (velocity amplitude) = 21.28 $\pm$ 0.16 km s^{-1}, e (eccentricity) = 0.5286 $\pm$ 0.0041, ω (angle of periastron) = 2.62 $\pm$ 0.81°, T_0 (time of periastron passage) = 2435319.73 $\pm$ 0.25 d, P (orbital period) = 178.3177 $\pm$ 0.0038 d, asin*i* (semimajor axis multiplied by the sin of the orbital inclination) = 43.3 $\times$ 10^6 km and Mass function = 0.1092. Figure 1.6 below shows the radial velocity curve their data produced, it can be seen that there is a significant amount of scatter in the data in the region of the trough which could be due to the star pulsating.

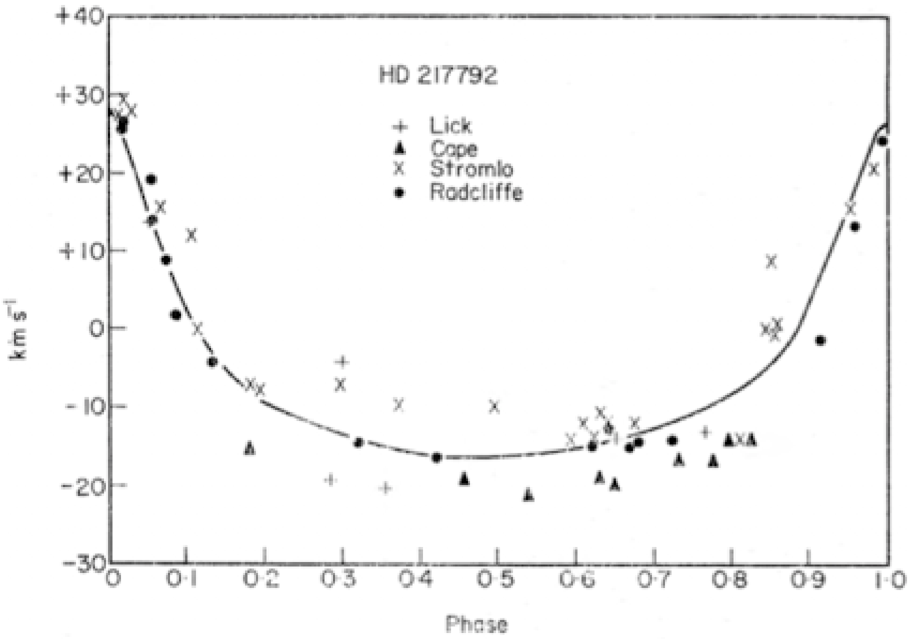

Figure 1.6: Radial velocity curve with orbital phase plotted against velocity with the fitted curve shown by the solid lines. Each of the different symbols denote each set of observations taken and labelled in the key, full details of these can be seen in [22]. Figure from [22].

An asterosesmic study carried out by V. Antoci et al 2019 [18], using data from the Transiting Exoplanet Survey Satellite mission sector 2, found six statistically significant pulsation frequencies: 0.6721(2), 1.0242(2), 1.2688(3), 1.3814(3), 1.6385(5) and 1.8376(3) d^{-1}. Further peaks were found in their analysis that were unable to be resolved as the data only spanned 27 days. From the peaks that were extracted there was no clear period spacing which shows that longer periods of observation are required for γ Dor pulsators [18].

This star was selected for this study due to the large number of spectroscopic observations available, 126 spectra, and the large number of photometric observations available, 3 TESS sectors. It was also deemed a suitable candidate due to being well studied in previously published literature, allowing this system to be used in order to develop the procedures used within this work.

1.4.2 HD 17310

HD 17310 is an F2 spectral class, dwarf luminosity class, γ Dor component of a single-lined spectroscopic binary star system. An asteroseismic study by Henry, Fekel & Henry 2005 [23] using photometric data found pulsation frequencies of: 0.4682 ± 0.0004, 0.5472 ± 0.0004, 0.4075 ± 0.0003 d^{-1} in the B band and 0.4673 ± 0.0003, 0.5488 ± 0.0004, 0.4083 ± 0.0002 d^{-1} in the V band. An orbital period of 27.793 days is suggested as the second best fit to their data as the best fit period of 0.9653 days is noted as being “spurious”.

A further study by R.F. Griffin, H.M.J. Boffin 2006 [24] found an orbital period of 27.67 ± 0.22 days, agreeing with the period suggested the previous year. Upon fitting their spectroscopic data, the following orbital parameters were determined: P (orbital period) = 27.819 ± 0.022 days, γ (systemic velocity) = +25.8 ± 0.7 km s^{-1}, K (velocity amplitude) = 24.0 ± 1.0 km s^{-1}, e (eccentricity) = 0.19 ± 0.04, ω (angle of periastron) = 125 ± 15°, T_0 (time of periastron passage) = MJD 53485.4 ± 1.2, $a_1 \sin i$ (semi-major axis multiplied by the sin of the orbital inclination) = 9.0 ± 0.4 Gm, Mass function = 0.038 ± 0.005 $M_\odot$. Figure 1.7 below displays the data used and the line of best fit obtained from the data used in the determination of these parameters.

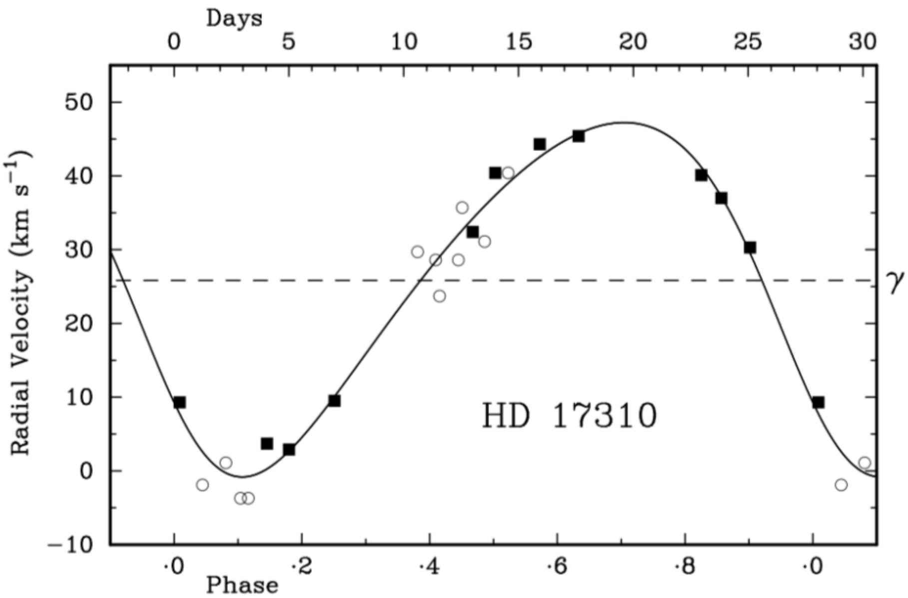

Figure 1.7: The radial velocity of HD 17310 plotted as a function of phase, with the fitted velocity curve plotted. R.F. Griffin, H.M.J. Boffin 2006 [24] observations are represented by the filled squares; those published by (Henry, Fekel & Henry 2005) are plotted as open circles. All were given equal weight in the solution of the orbit. Figure taken from [24].

This star was selected for this study due to the large number of spectroscopic observations available, 91 spectra, and the large number of photometric observations available, 2 TESS sectors. It was also deemed a suitable candidate due to being well studied in previously published literature, allowing for a meaningful comparison of results.

1.4.3 HD 85964

HD 85964 is an ellipsoidal variable, a star with a higher mass companion distorting the shape of the primary star leading to variations in its apparent brightness, and component in a single-lined spectroscopic binary star system with orbital parameters: P (orbital period) = 1.24850 days, e (eccentricity) = 0.0, K (velocity amplitude) = 65.5(5) km s^{-1}, $a_1 \sin i$ (semi-major axis multipled by the sin of the orbital inclination) = 0.00752(6) AU and Mass function = 0.0364(8). The data used in the determination of these parameters and the fitted radial velocity curve can be seen below in figure 1.8

[26]. This system has also been classified as an eclipsing binary system by Eyer et al 2002 as seen in [26] due to their observation of differing depths of successive minima in the light curves. Further study on this system determined the following stellar parameters: T_{eff} (effective temperature) = 6600 ± 220 K, log g = 4.14 $\pm$ 0.13 and [M/H] (metallicity) = +0.11$\pm$ 0.11 [26].

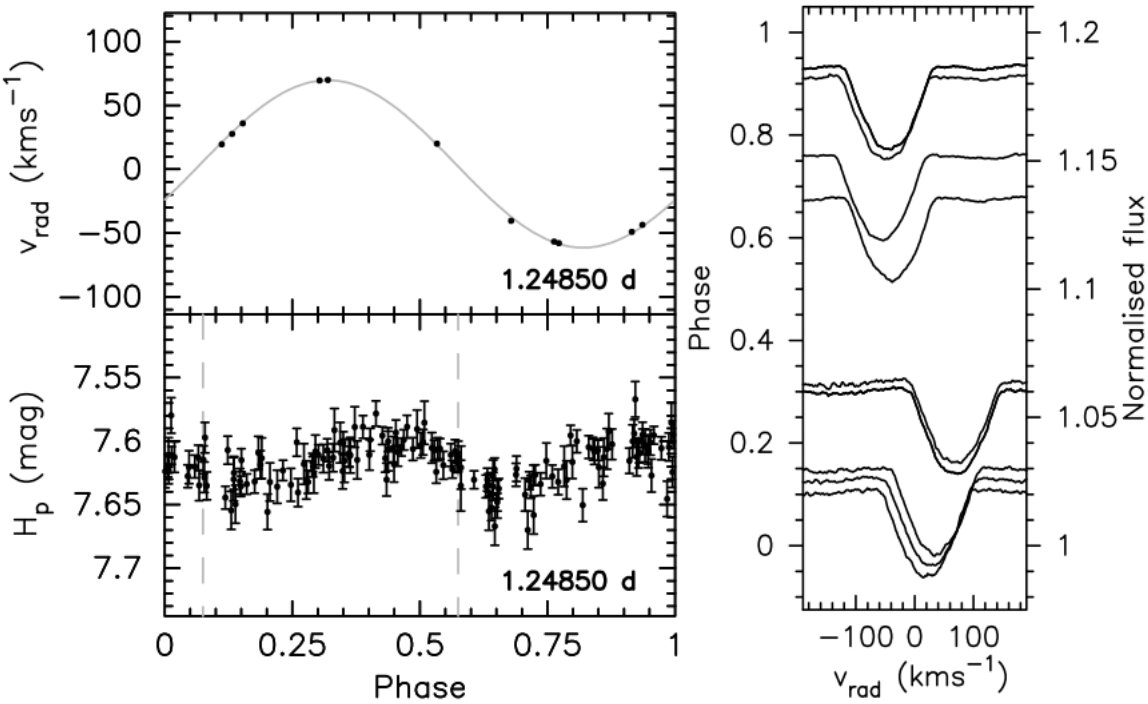

Figure 1.8: Phase plotted against radial velocity v_{rad} (*top left*) and the Hipparcos H_p measurements (*bottom left*) of HD 85964 with the period given in the bottom right corner. The reference time is HJD 2450000. The dashed lines in the bottom left panel show the phase at which $v_{rad} = v\gamma$. On the right, observed cross-correlation profiles are plotted against orbital phase. Figure is taken from [25].

This star has been selected for use in this study as the variability exhibited is directly linked to the binary motion of the star, being both an ellipsoidal variable and eclipsing binary. This makes it an ideal comparison star for determining the reliability of the results obtained for the two selected variables.

1.5 Observational Techniques

Two techniques will be explored and utilised in this work in order to undertake asteroseismic analysis of the selected SB_1 systems: photometric analysis of TESS data and radial velocity analysis of spectroscopic data. From these two data sets both the frequency and mode of pulsation can be determined, providing valuable insight into the stars interior structure.

1.5.1 Photometry using TESS

The *Transiting Exoplanet Survey Satellite*, TESS [27], follows on from the mission of *Kepler* aiming to expand to the search for transiting exoplanets. By utilising a high-Earth elliptical orbit, with a period of 13.7 days, a stabler platform is provided for precise photometry, compared to the low-Earth orbit that had formed the basis of previously proposed missions. The aim of the original mission of TESS was to create an all-sky survey, by observing the sky in sectors for equal periods of time, 27 days. The pattern and duration of the initial missions' observations is illustrated below in Figure 1.9. Despite the main aim of the mission being to detect and catalogue exoplanets, it also provides excellent data for photometric analysis. It was designed to be able to detect a broad range of exoplanet orbital periods, ranging from a few hours to over a year, making it ideal for observing both the high frequency p-mode and low frequency g-mode pulsations of variable stars. For selected stars a short cadence of 2 minutes is used for observations. This enables these observations to be used for asteroseismology [27] with other cadences being available as well.

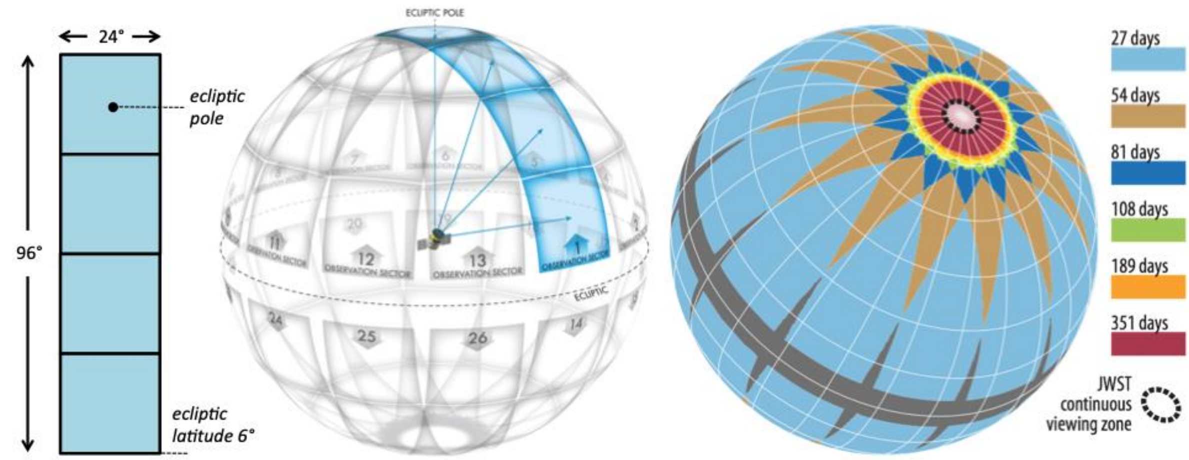

Figure 1.9: a schematic of: left – the instantaneous field of view of the four TESS cameras combined, centre – the projection of the 26 observing sectors on the celestial sphere, right – the consecutive observation duration projected onto the celestial sphere, highlighting the overlap between sectors. This shows the viewing sectors for the original TESS mission which has since been extended, the size and shape of the viewing sectors for the extended mission remain the same but their sky positions have changed. Image from [27].

1.5.2 Spectroscopic analysis

Spectroscopy not only allows for the determination of a whether a star exists as part of a binary star systems, as discussed earlier in 1.1.4, it also allows for asteroseismic analysis of the stars to be undertaken as well. Currently only ground-based spectroscopic observations can be carried out at sufficiently high resolutions for this analysis to be carried out. The raw data is first reduced, dark current removal, offset and bias correction, sky background subtraction and, wavelength calibration is the usual procedure followed for data taken from most spectrographs (this can vary between each instrument, but the basic procedure remains largely the same). In the case of asteroseismology, the wavelength calibration and flat-fielding require a very high level of accuracy throughout the duration of the star's oscillation cycle. From this we are able to plot a graph of wavelength against normalised flux where peaks can be seen at specific wavelengths. We aim for a relatively high signal-noise ratio to allow for the study of the star's oscillations from line profile variations. Isolated lines of a star's spectrum are referred to as line profiles. When the shape of a line profile varies over time, it is referred to as a line profile variation; this can be seen below in Figure 1.10 [8].

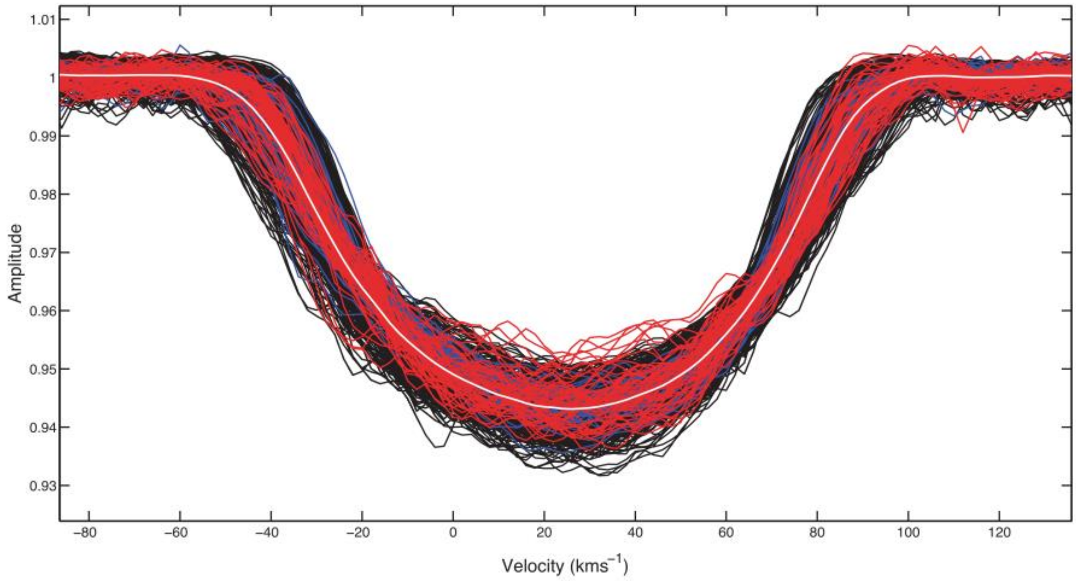

Figure 1.10: Scaled line profiles of the three data sets. McDonald (red), La Silla (blue) and MJUO (black) observations are shown with the mean line profile (white). Figure taken from [28].

1.6 Aims of Research

The aim of this work is to apply asteroseismic analytical techniques to single-lined spectroscopic binary star systems in order to determine pulsation frequencies from both photometric and spectroscopic observations of the three selected systems. Existing analytical techniques can be applied directly to the TESS photometry data available. Additional steps can be taken to remove the effects of the Doppler shift caused by the binary motion of the stars in the spectroscopic data, by modelling the stars binary motion and subtracting this from the observed velocities, and then asteroseismic analysis techniques can be applied to the resulting line profiles. These independent determinations of pulsation frequencies can then be compared to determine the agreement between the values obtained using two separate data sources.

2. Methodology

For each star a set of pulsation frequencies from TESS photometry will be determined. These will then be compared to the frequencies obtained through analysis of spectroscopic line profiles, after the binary orbit has been modelled and removed.

2.1 Photometric Analysis

TESS light curves were accessed via the Mukulski Archive for Space Telescopes (MAST) [29]. The Lightkurve package [30] was used in order to download and inspect the light curves of the three selected SB_1 systems. The TESS light curves were downloaded and the sector data with the author TESS Science Processing Operations Centre (SPOC) was imported. SPOC takes the full-frame images captured by TESS, with a 1800s cadence (30 minutes), and calibrates them; this is done in order to produce calibrated pixels, light curves and centroids for all of the missions target stars. Systematic errors are then removed from the images through the use of Pre-search Data Conditioning Simple Apature Photometry (PDCSAP) [29]. Each available sector of data for the target stars was then analysed using the following procedure individually. This was done to allow for the identification of any anomalies present within individual light curves. Fitting periodic signals over data with larger time differences would introduce significant errors into the determined pulsation frequencies.

The 120s cadence sector data was downloaded and plotted. Pyriod [31] was then imported and utilised to generate a periodogram, an example of which can be seen below in figure 2.1, a Fourier transform amplitude spectrum, from the light curve. Stellar pulsations are periodic due to them occurring at the stars "eigenfrequencies". These cannot be easily seen when a light curve is viewed in the time domain; by utilising Fourier transforms these frequencies can now be visualised. From the plotted periodogram, frequencies were identified by pyriod as it highlights the peak with the greatest amplitude. Peaks are added until the solution resembles the shape of the light curve, and no periodicity can be seen in the residuals, this is the pre-whitening process. Multiples (harmonics) or combinations of lower frequencies were removed from the data set until the base frequencies were identified. The frequencies found for each sector of data were then averaged and associated error calculated. It is assumed that the frequencies are not changing between sectors.

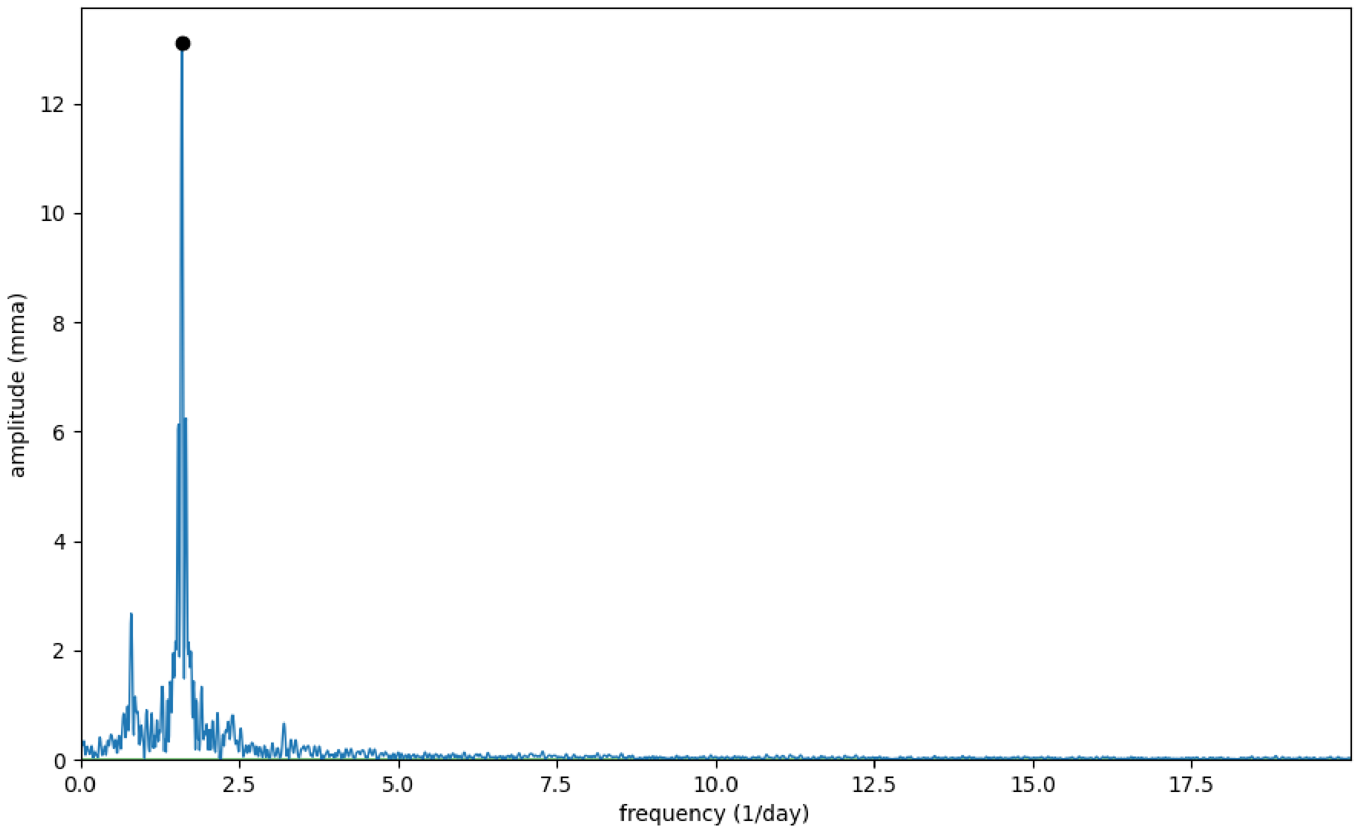

Figure 2.1: Fourier Transform of TESS Sector 35, 120s cadence, light curve of HD 85964, a non-pulsator generated using pyriod. The solid black circle indicates the peak with the highest amplitude at a frequency of 1.6 d^{-1}.

2.2 Spectroscopic Analysis

Spectra of the target stars from the University of Canterbury Mt John Observatory (UCMJO) in New Zealand were collected using the 1 m McLellan telescope with the fibre-fed High Efficiency and Resolution Canterbury University Large Echelle Spectrograph (HERCULES) with a resolving power of R = 50 000 operating over a range of 3800–8000 Å [32]. MEGARA was used for the reduction of the data, a semi-automated MATLAB based method [33]. The procedure produces a normalised, order merged and wavelength calibrated set of spectra. It also applies a barycentric correction and cosmic ray removal in order to prepare the data for analysis [28]. This preprocessing was carried out by Dr Emily Brunsden and the following analysis was carried out as part of this work.

The available spectra were plotted with velocity against intensity in order to visualise the range of radial velocities present within the set of line profiles. The mid-point of the trough was calculated by taking an average of the velocity values at the same intensity over a specified velocity range. These were then averaged in order to determine the mid-point velocity of an individual line profile. This method was used as the line profiles are not symmetrical so were unsuitable for Gaussian fitting. The radial velocity from the previous stage was then plotted as a function of time to generate the radial velocity curve of the star.

StarSolve [34], a program designed and used in the radial velocity fitting of both single-lined and double-lined spectroscopic binary star systems radial velocity curves, was then utilised in order to fit the RV and obtain the star's orbital parameters. In brief, the code performs this fit by: averaging the radial velocity data to determine the systemic velocity, estimate the velocity amplitude by taking the difference between the maximum and minimum radial velocities and diving this by 2, calculates the orbital period by averaging the separation between maxima and minima, iterates eccentricity from 0.01 to 0.99 in steps of 0.01 and for each of these values and finds values for the angle of periastron and the time of periastron passage until it reaches the smallest possible residuals, having little to no variation, and returns the parameters used to achieve this starting estimate [34]. This is followed by the program using a chi-squarered minimisation followed by the Levenberg-Marquardt algorithm in order to provide the fit.

The fitted orbital parameters were then used to calculate the expected radial velocity of the star if it was not pulsating; these expected radial velocities are then subtracted from the observed radial velocity in order to shift the line profiles and remove the effects of the Doppler shift from the binary motion.

These corrected line profiles are then imported into FAMIAS (Frequency Analysis and Mode Identification for Asteroseismology) [35] where a 1-D mean Fourier transform is generated from the time series of spectra; from this, peak frequencies can be identified and as above screened for aliases in order to determine the base pulsation frequencies for the star.

2.3 Determining the reliability of Results

The reliability of the results obtained will be determined through the comparison of the results obtained through both photometric and spectroscopic analysis. These results will also be compared to results obtained by previous photometric and spectroscopic studies. These comparisons of results will determine how useful the binary modelling method is in order to determine the stars pulsation frequencies.

3. Results and Discussion

3.1 π PsA (HD 217792)

The following are the pulsation frequencies determined through the use of both photometric and spectroscopic observations of HD 217792 accompanied by previously published frequencies to determine the reliability of the results obtained during this study. This star has been included in the study due to the wealth of previously published information as well as being included in three sectors of TESS observations and having 126 spectroscopic observations.

3.1.1 Photometric Analysis

Presented below are the results obtained during the photometric analysis of the light curves of HD 217792.

Table 3.1: Pulsation frequencies from TESS photometry data of HD 217792, averaged over three sectors (2, 28 and 69), with their respective error, the standard deviation (σ) of the individual results and previously published results obtained using data from sector 2 with errors in parentheses.

Frequency/d^{-1}	Error/d^{-1}	σ	Frequency/d^{-1} V. Antoci, 2019 [18]
0.670	0.002	0.009	0.6721(2)
1.025	0.001	0.004	1.0242(2)
1.278	0.002	0.023	1.2688(3)
1.3813	0.0007	0.026	1.3814(3)
1.639	0.002	0.004	1.6385(5)
1.840	0.003	0.009	1.8376(3)

As shown above in table 3.1, it can be seen that π PsA has 6 base pulsation frequencies with all, excluding the third, agreeing with the results published by V. Antoci et al 2019 [18] within their respective errors. The third identified frequency, $1.278 \pm 0.002\ d^{-1}$, has the second highest standard deviation for the frequencies determined from each sector of TESS data, with the frequency determined from the observation of sector 28 having the greatest difference; the source of this variation between the determined frequencies will require further work beyond the scope of this study. The previously published results include one observed sector, the second sector of the original TESS mission, and the ones presented from this study are an average taken from sector 2, 28 and 69 using 120s cadence data. Further analysis will be required in order to determine if the assumption that the frequencies do not change between sectors is valid due to the standard deviation being significantly larger than their errors; this can be tested in further work when more sectors of data are made available.

3.1.2 Spectroscopic Analysis

Shown below in figure 3.1 are 128 line profiles with variation caused by both the Doppler shift, as the two stars orbit each other, and the pulsations of the primary star. It can be seen that a significant number of these line profiles appear to overlap in the –20 to 0 km s^{-1} range with very few exceeding these velocities. This is due to the approximately 60 day period over which the observations were carried out.

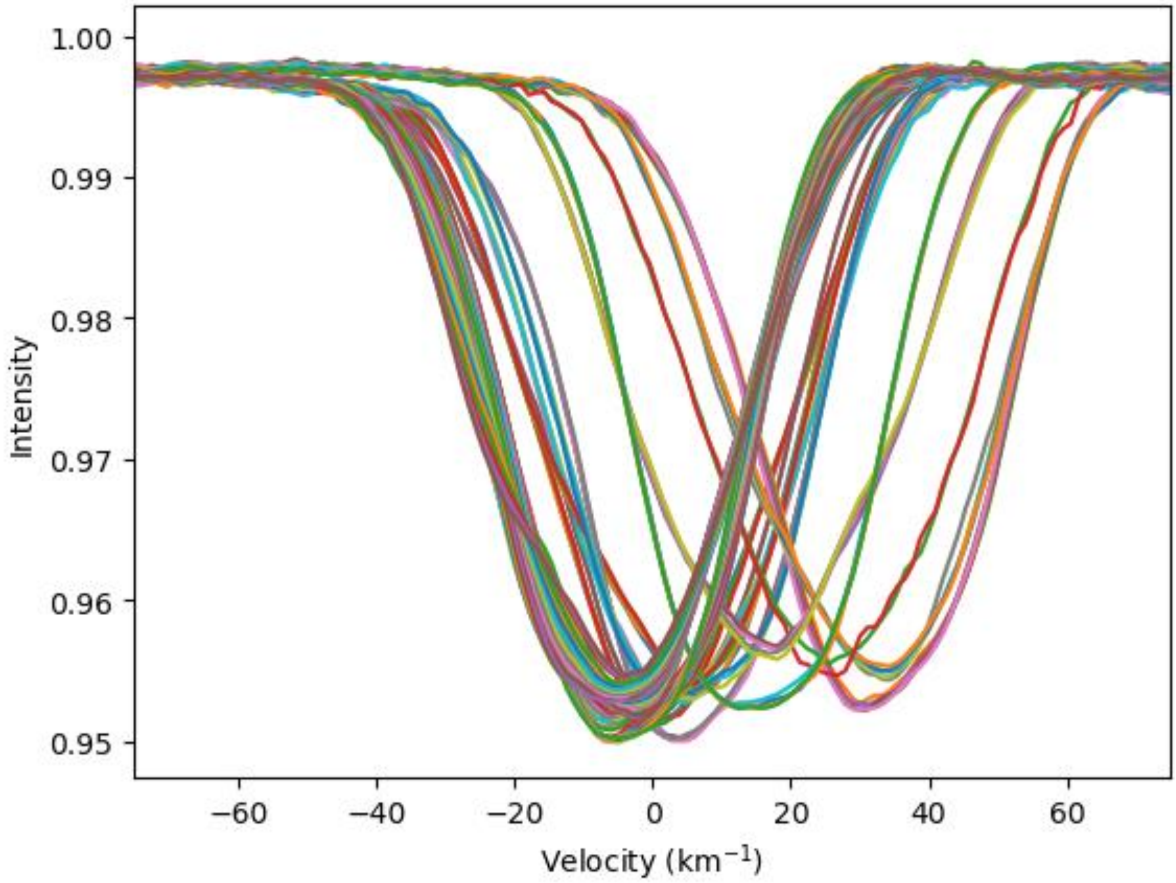

Figure 3.1: Line profiles for SB_1 spectroscopic binary HD 217792, a γ Dor pulsator. Each line represents a single observation and the variations in the velocities for each line are the result of both stellar pulsations, affecting the shape, and binary motion, affecting the position.

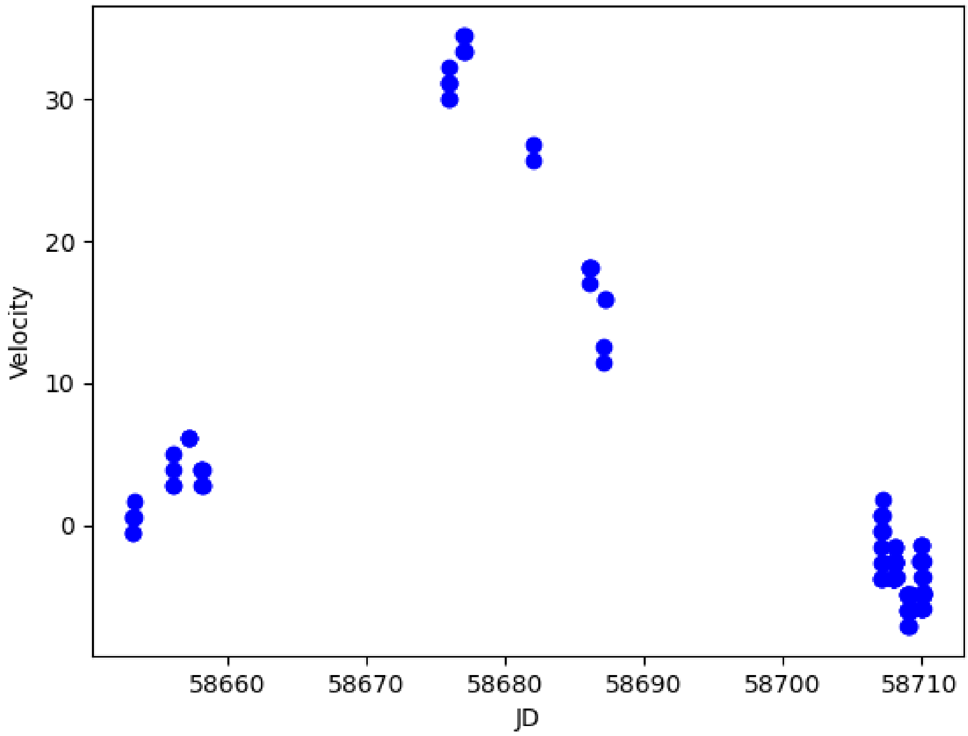

Figure 3.2: Radial Velocity curve for HD 217792, produced using above spectroscopic data. The velocity is measured in km s^{-1}. The Julien Date (JD) displayed is in a shortened form, 2500000 has been subtracted, for clarity.

The RV curve produced from the above spectroscopic data, figure 3.2, proved to be insufficient to use on its own for orbital fitting as the data range spans approximately one third of the binary orbital period, 178.3177 $\pm$ 0.0038 days [22]. In order to obtain a fit to be used in further analysis, data from Bopp et al 1970 [22] was combined with the above data to produce a completed RV curve, as shown below in figure 3.3.

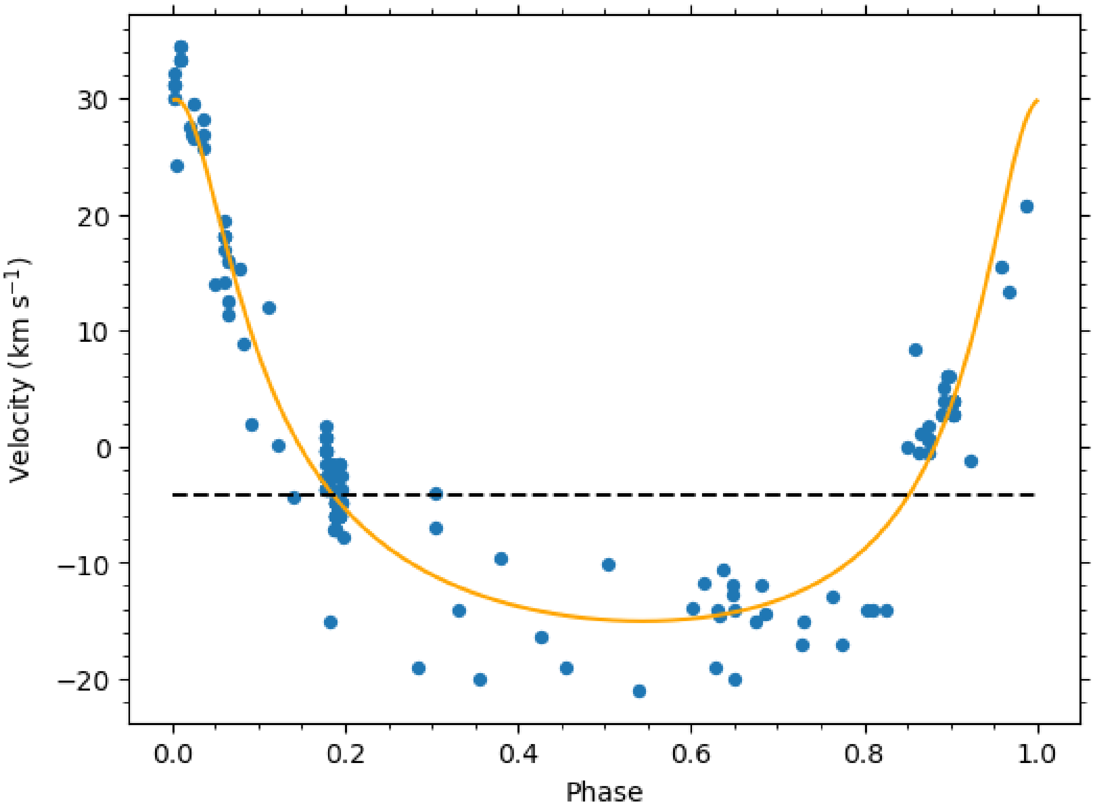

Figure 3.3: Radial Velocity curve for HD 217792, plotting orbital phase against velocity with the best fit shown by the orange line. Data is a combination of the data above and data taken from Bopp et al 1970 [22]. Orbital phase is plotted against radial velocity for clarity and better visualisation of the quality of the fit. Error bars for this data are too small to be seen.

The orbital parameters obtained during the fitting process, shown below in table 3.2, were used to remove the effect of the star existing within a binary star system to leave only variations in the radial velocity caused by the stellar pulsations. The corrected line profiles can be seen below in figure 3.4, they align much more closely with each other and are centred about 0 on the x-axis.

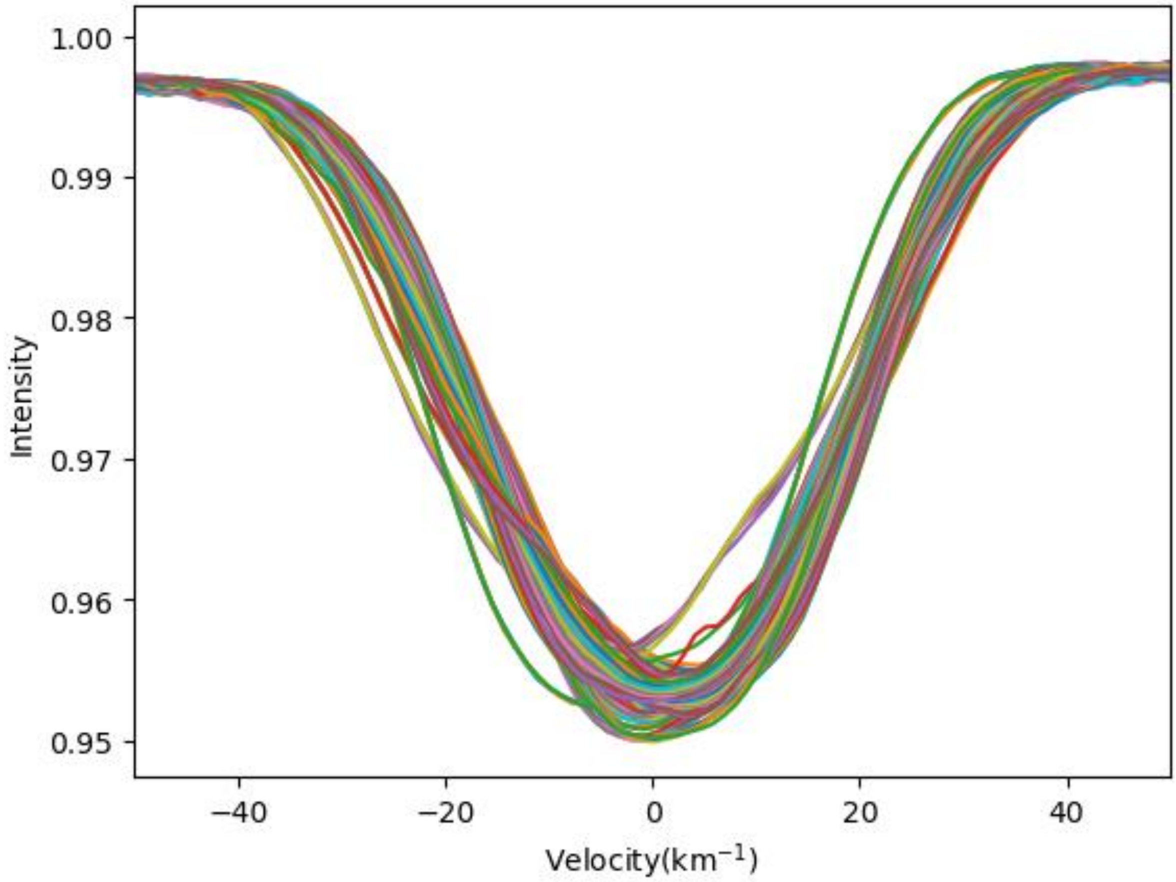

Figure 3.4: Corrected line profiles for HD 217792 showing the variations caused by stellar pulsations. With the binary motion removed the velocity variations are a direct result of the pulsations of the star.

Table 3.2: Fitted orbital parameters from the Radial Velocity curve of HD 217792 with previously determined orbital parameters for comparison to determine the quality of the fit.

Parameter	This work	B. W. Bopp et al 1970 [22]
γ (km s^{-1})	-4.2292	-5.97 ± 0.11
K (km s^{-1})	22.475	21.28 ± 0.16
e	0.52126	0.5286 ± 0.0041
ω (°)	354.13	2.62 ± 0.81
T_0	58675.5	2435319.73 ± 0.25
A sin*i* ($\times 10^6$ km)	47.027	43.3
Mass function	0.13036	0.1092
P (days)	178.302	178.3177 ± 0.0038

As seen above in table 3.2, discrepancies can be seen between the previously published orbital parameters and the results obtained in this work whilst both providing, upon visual inspection, a good fit to the data present. This could be due to the vast time difference between the observations and the larger scatted in the trough region in figure

3.3. This can also be attributed to stellar pulsations altering the observed radial velocity and the measured radial velocities not solely being caused by the stars orbital motion.

Table 3.3: Pulsation frequencies from FAMIAS analysis of spectroscopic observation of HD 217792.

	Frequency/d^{-1}	Relative Amplitude	S/N ratio
F_1	0.661(1)	0.12(3)	9.147
F_2	1.018(1)	0.16(2)	8.131
F_3	1.278(2)	0.11(2)	4.753
F_4	1.373(1)	0.12(2)	6.224
F_5	1.625(2)	0.12(2)	7.231
F_6	1.838(2)	0.10(2)	4.774

Presented above in table 3.3 are the results of the FAMIAS analysis of the 128 line profiles for HD 217792. Six pulsation frequencies were identified during this process all with a signal-noise ratio above 4.7 and a relative amplitude in the range of 0.10 to 0.16.

3.1.3 Comparison of Results

Table 3.4: Summary of calculated pulsation frequencies for HD 217792 calculated from both photometric and spectroscopic analysis.

$Frequency_P/d^{-1}$	$Frequency_S/d^{-1}$
0.670(2)	0.661(1)
1.025(1)	1.018(1)
1.278(2)	1.278(2)
1.3813(7)	1.373(1)
1.639(2)	1.625(2)
1.840(3)	1.838(2)

As seen above in table 3.4, it can be seen that the third and the highest pulsation frequencies obtained agree within error between the two data sources. Whilst being close, the values obtained during the spectroscopic analysis lie outside the margin of error for the results obtained during photometric analysis. This could be due to the significant difference in the number of data points used in the determination of the pulsation frequencies. In order to ascertain which of the values lie closer to the true pulsation frequencies of this star a longer period of continuous observation is required both photometrically and spectroscopically. The current longest continuous photometric observation of this star spans just below one seventh of the binary orbital period and the longest continuous spectroscopic observation spans approximately one third of the stars binary orbital period. With all of the frequencies obtained through both techniques being similar, further work on the procedure used in the spectroscopic analysis could yield results agreeing with the error of each determined frequency.

3.2 HD 17310

The following are the pulsation frequencies determined through the use of both photometric and spectroscopic observations of HD 17310 accompanied by previously published frequencies to determine the reliability of the results obtained during this study. This star has been selected for use in this study due to the high number of spectroscopic observations, 91, available for analysis and that there are two available sectors of TESS observations.

3.2.1 Photometric Analysis

Presented below are the results obtained during the photometric analysis of the light curves of HD 17310.

Table 3.5: Pulsation frequencies from TESS photometry data of HD 17310, averaged over 2 sectors (4 and 31), with their respective error, σ and previously published results.

Frequency/d^{-1}	Error/d^{-1}	σ	Frequency/d^{-1} B band [23]	Frequency/d^{-1} V band [23]
0.403	0.004	0.006	0.4075 ± 0.0003	0.4083 ± 0.0002
0.453	0.006	0.008	0.4682 ± 0.0004	0.4673 ± 0.0003
0.558	0.003	0.004	0.5472 ± 0.0004	0.5488 ± 0.0004

As shown above in table 3.5, 3 base pulsation frequencies are identified from the light curves of HD 17310, with only the second frequency agreeing with the results published by Henry, Fekel & Henry 2005 [23] completely within their respective errors. The first frequency is very close to agreement with the pulsation frequency identified by Henry, Fekel & Henry 2005 [23] in the B photometric band and there is a more significant discrepancy between the third frequency identified in this work and the previously published frequency. In order to determine the source of this discrepancy further extended analysis would need to be carried out beyond the scope of this study. The pulsation frequencies determined as part of this work used data from sector 4 and 31 of the TESS mission. When HD 17310 is observed again in future TESS sectors, this analytical procedure can be repeated, and the results included in these average frequencies in order to reduce the error in the values. Further analysis will be required in order to determine if the assumption that the frequencies do not change between sectors is valid due to the standard deviation being significantly larger than their errors; this can be tested in further work when more sectors of data are made available.

3.2.2 Spectroscopic Analysis

Shown below in figure 3.5 are 91 line profiles that exhibit variation due to both the pulsations of the primary star and the Doppler shift caused by the binary orbital motion of the two stars in the system. The mid-point velocity for each of these profiles was calculated using the moment method and then used to plot a radial velocity curve.

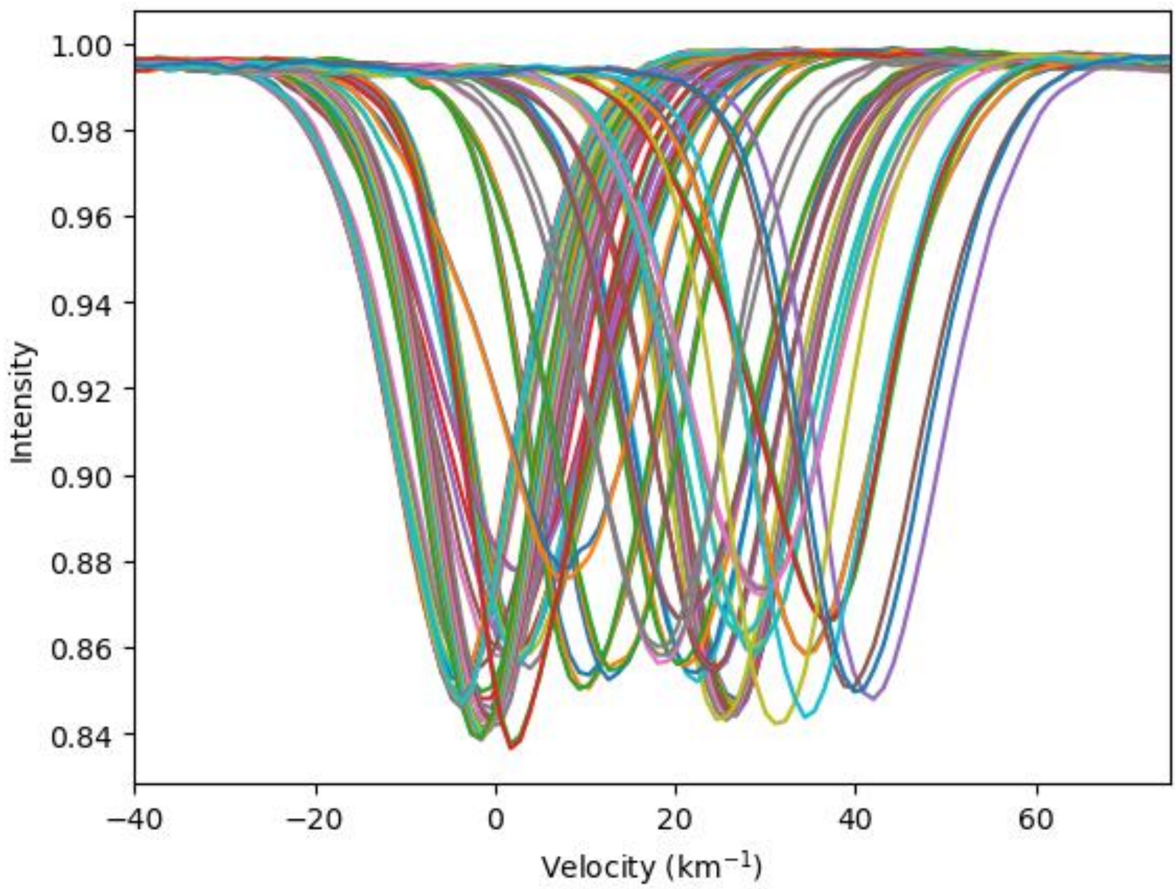

Figure 3.5: Line profiles for SB_1 spectroscopic binary HD 17310, a γ Dor pulsator. The velocity is measured in km s^{-1}. Each line represents a single observation and the variations in the velocities for each line are the result of both stellar pulsations and binary motion.

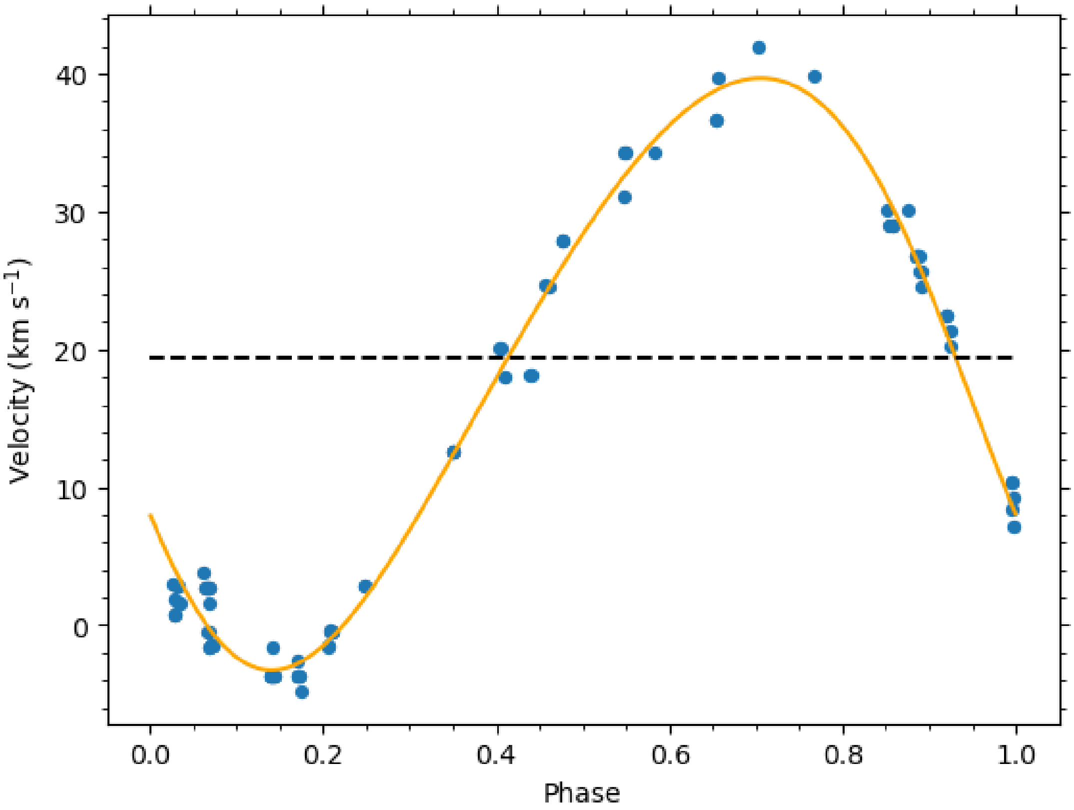

Figure 3.6: Radial Velocity curve for HD 17310, plotting orbital phase against velocity with the best fit shown by the orange line. Orbital phase is plotted against radial velocity for clarity and better visualisation of the quality of the fit. Error bars for this data are too small to be seen.

The orbital parameters obtained during the fitting process, shown below in table 3.6, were used to remove the effect on the radial velocity of the star existing within a binary star system to leave only variations in the radial velocity caused by the stellar pulsations. As opposed to the fit presented in figure 3.3, the orange fit line in figure 3.6 aligns much more closely with the data points. The corrected line profiles can be seen below in figure 3.7, they align much more closely with each other and are centred about 0 on the x-axis.

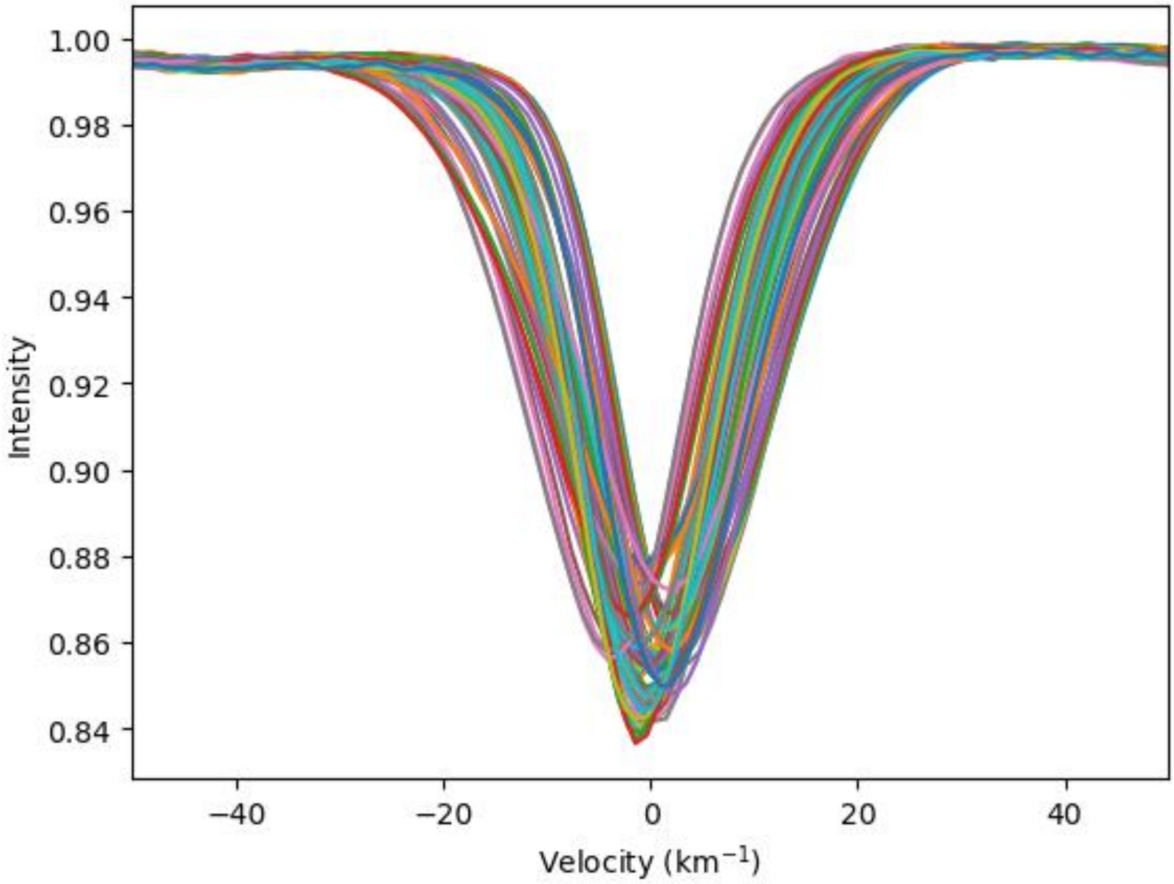

Figure 3.7: Corrected line profiles for HD 17310 showing the variations caused by stellar pulsations. The velocity is measured in km s^{-1}. With the binary motion removed the velocity variations are a direct result of the pulsations of the star.

Table 3.6: Fitted orbital parameters from the Radial Velocity curve of HD 17310 with previously determined orbital parameters for comparison to determine the quality of the fit.

Parameter	This work	R.F. Griffin, H.M.J. Boffin 2006 [24]
γ (km s^{-1})	19.39	25.8 ± 0.7
K (km s^{-1})	21.473	24.0 ± 1.0
e	00.11611	0.19 ± 0.04
ω (°)	188.21	125 ± 15
T_0	58361	53485.4 ± 1.2
A sin*i* (× 10^6 km)	8.1714	9.0 ± 0.4
Mass function	0.028008	0.038 ± 0.005
P (days)	27.8624	27.819 ± 0.022

Similarly, to the fit provided for HD 217792, it can be seen above in table 3.6 that there are discrepancies between the previously published orbital parameters and those found during this work. These discrepancies between the two sets of orbital parameters could be attributed to stellar pulsations causing the individual radial velocity measurements to differ from the radial velocity caused only by the stars orbital motion.

Table 3.7: Pulsation frequencies from FAMIAS analysis of spectroscopic observations of HD 17310.

	Frequency/d^{-1}	Relative Amplitude	S/N ratio
F_1	0.404(1)	0.30(7)	2.872
F_2	0.455(1)	0.3(1)	3.586
F_3	0.544(8)	0.5(1)	5.251

Presented above in table 3.7 are the results of the FAMIAS analysis of the 91 line profiles for HD 17310. Three pulsation frequencies were identified during this process all with a S/N ratio above 2.8 and a relative amplitude in the range of 0.3 to 0.5.

3.2.3 Comparison of Results

Table 3.8: Summary of calculated pulsation frequencies for HD 17310 calculated from both photometric and spectroscopic analysis.

$Frequency_P/d^{-1}$	$Frequency_S/d^{-1}$
0.403(4)	0.404(1)
0.453(6)	0.455(1)
0.558(3)	0.544(8)

As shown above in table 3.8, only the first and second pulsation frequencies identified agree within error between the two sources of data. Whilst the two sets of results are very similar, the other identified frequency lies outside of the margin of error of the photometrically determined pulsation frequency. The discrepancies between the results obtained could be attributed to the discrepancies seen above in table 3.6 between the fitted orbital parameters. The fitting procedure does not account for variation in radial velocity measurements caused by stellar pulsations. Further spectroscopic and photometric observations of this star are required in order to more accurately determine the pulsation frequencies and reduce the discrepancies between the two sets of frequencies.

3.3 HD 85964

The following are the pulsation frequencies determined through the use of both photometric and spectroscopic observations of HD 85964, this star was a previous γ Dor candidate but has since been classified as an ellipsoidal variable and potential eclipsing binary [26]. It has been included in this study for comparative purposes to illustrate the difference in results obtained between true pulsators and stars exhibiting variability from other sources.

3.3.1 Photometric Analysis

Presented below are the results obtained during the photometric analysis of the light curves of HD 85964.

Table 3.9: Frequencies identified from TESS photometry data of HD 85964, averaged over 4 sectors (35, 36, 62 and 63), with their respective error and σ.

Frequency/d^{-1}	Error/d^{-1}	σ
0.8008	0.0001	0.0002
1.60200	0.00002	0.00004
2.4029	0.0002	0.0004
3.2036	0.0004	0.0007

From photometric analysis of the four 120s cadence light curves for HD 85964, the four frequencies identified are shown above in table 3.9. the last three frequencies are all harmonics of the lowest frequency identified. When the light curves are folded about this frequency clear periodicity can be seen, as illustrated below in figure 3.8. This frequency is the same as the binary orbital period, 1.24850 days published previously [25] and 1.248751 days determined from this work, 0.8008 d^{-1}. This sinusoidal variation coinciding with the binary orbital period confirms this classification of this star as an ellipsoidal variable. Further analysis will be required in order to determine if the assumption that the frequencies do not change between sectors is valid due to the standard deviation being significantly larger than their errors; this can be tested in further work when more sectors of data are made available.

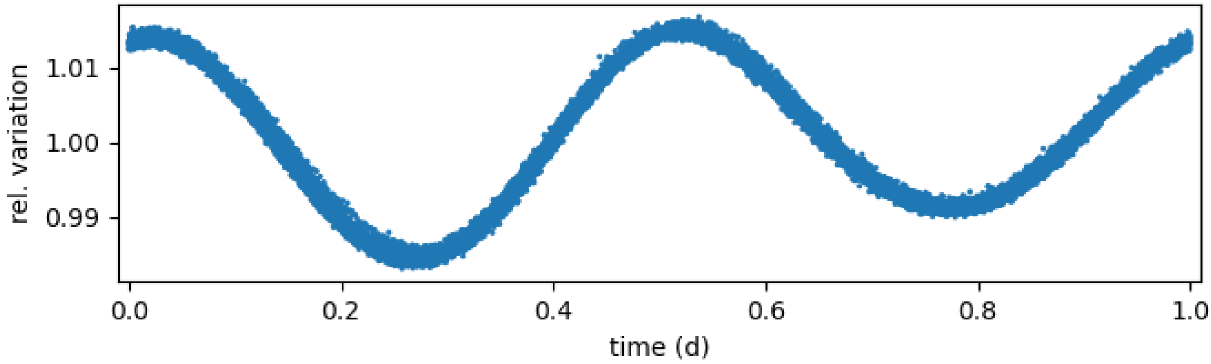

Figure 3.8: TESS light curve, sector 63, of HD 85964 folded about the frequency 0.8008 d^{-1}, corresponding with the orbital period of 1.248751 days. Clear sinusoidal variation can be seen as well as the differing depths of successive minima noted by Eyer et al 2002 as seen in [26].

3.3.2 Spectroscopic Analysis

Shown below in figure 3.9 are 45 line profiles exhibiting variation in velocity measurements due to both the stars orbital motion and ellipsoidal variability. The mid-point velocity of these line profiles was used in order to obtain the radial velocity values used in plotting the radial velocity curve shown below in figure 3.10.

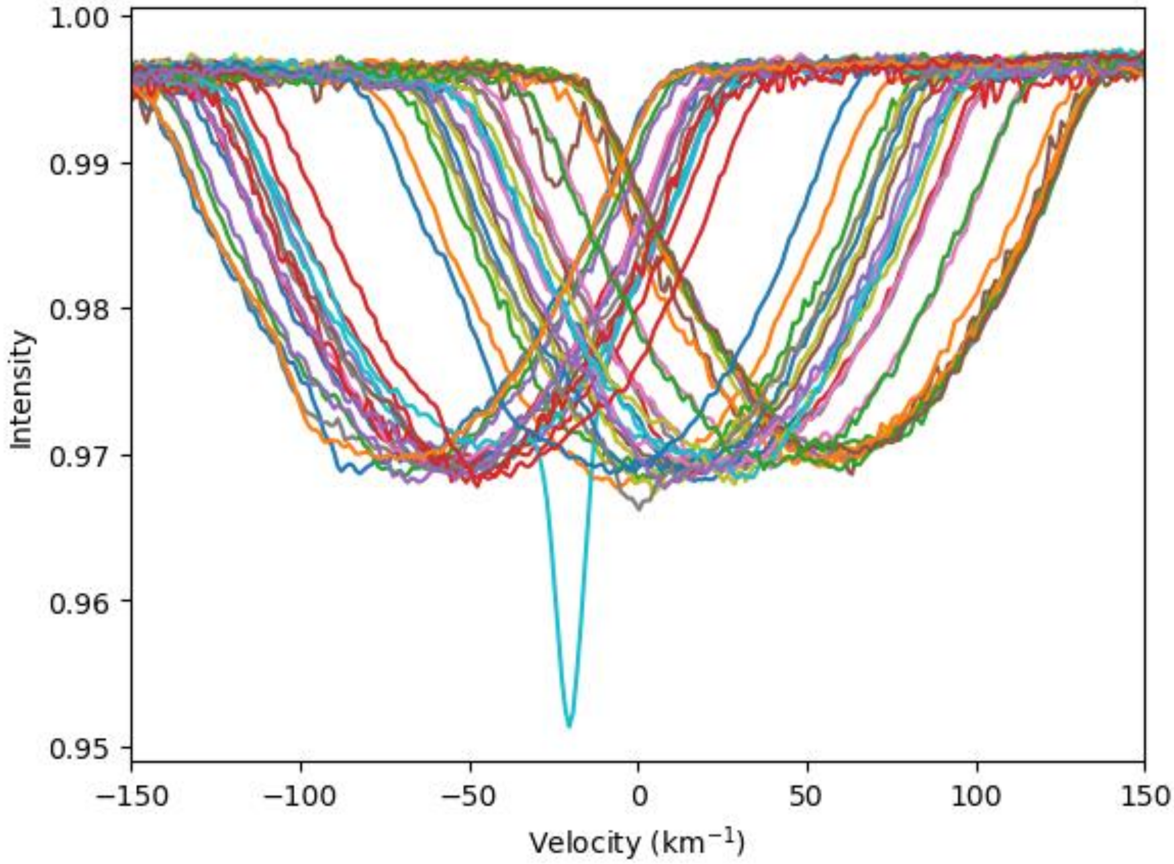

Figure 3.9: Line profiles for SB_1 spectroscopic binary HD 85964, an elliptical variable. The velocity is measured in km s^{-1}. Each line represents a single observation and the variations in the velocities for each line are the result of both the ellipsoidal effect and binary motion. The sharp peak in turquoise is likely a spurious spectrum not of this star or there is an anomaly that occurred during the collection of the spectrum.

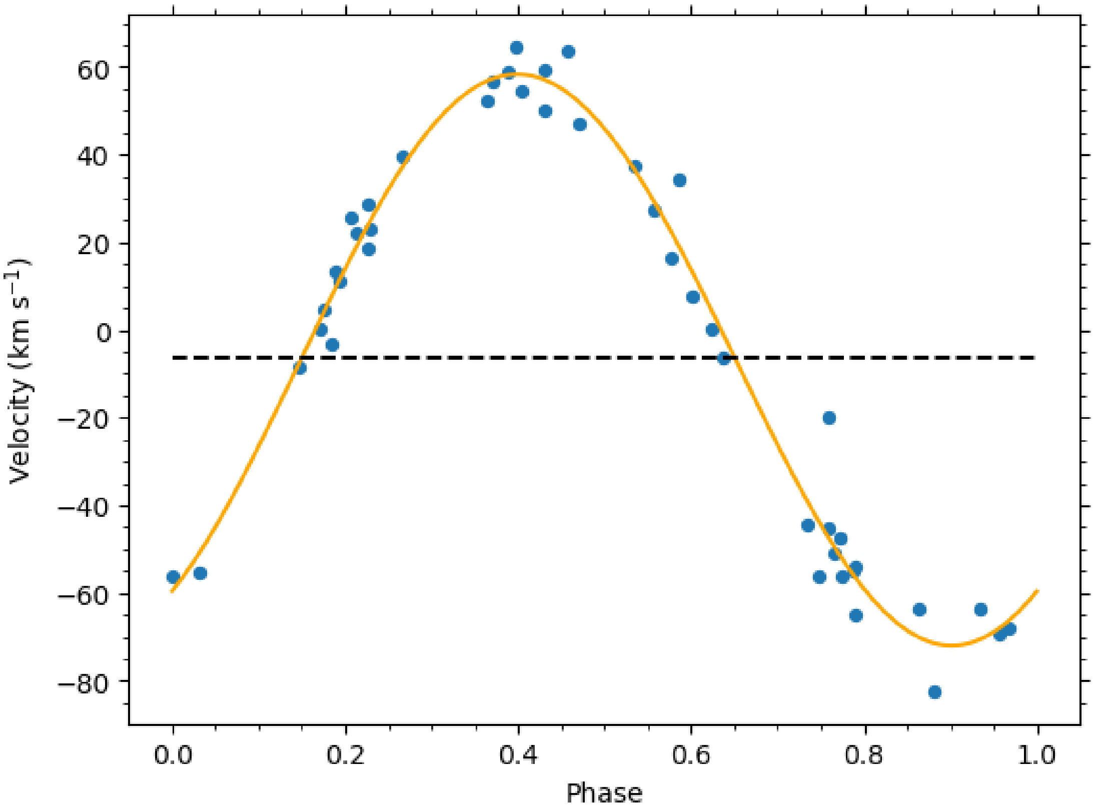

Figure 3.10: Radial Velocity curve for HD 85964, plotting orbital phase against velocity with the best fit shown by the orange line. Orbital phase is plotted against radial velocity for clarity and better visualisation of the quality of the fit. Error bars for this data are too small to be seen.

The orbital parameters obtained during the fitting process, shown below in table 3.10, were used to remove the effect on the radial velocity of the binary motion of the star to leave only variations in the radial velocity caused by the ellipsoidal effect The corrected line profiles can be seen below in figure 3.11, they align much more closely with each other, compared to those in figure 3.9, and are centred about 0 on the x-axis.

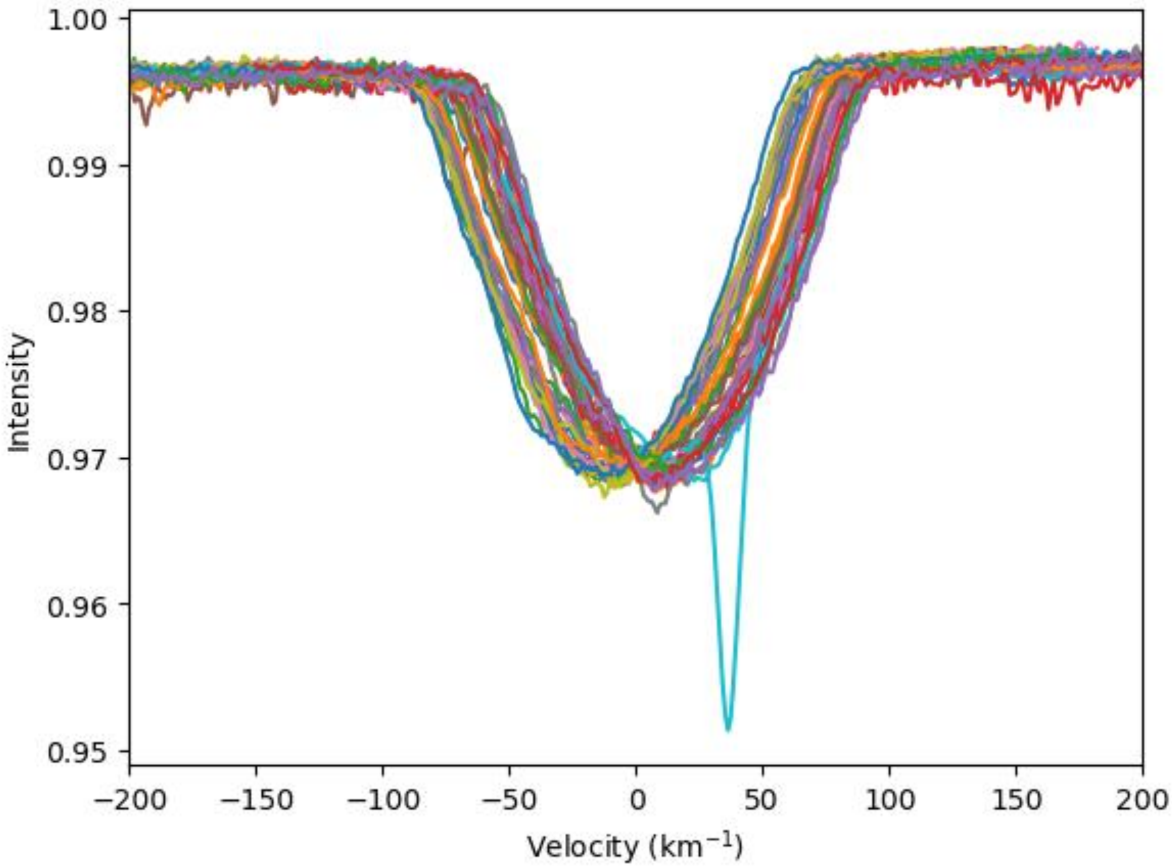

Figure 3.11: Corrected line profiles for HD 85964 showing the variations caused by elliptical variation. The velocity is measured in km s^{-1}. With the binary motion removed the velocity variations are a direct result of the ellipsoidal effect, a higher mass secondary star causing a distortion to the shape of the primary star leading to periodic variations in the apparent brightness corresponding to the orbital period. The sharp peak in turquoise is likely a spurious spectrum not of this star or there is an anomaly that occurred during the collection of the spectrum.

Table 3.10: Fitted orbital parameters from the Radial Velocity curve of HD 17310 with previously determined orbital parameters for comparison to determine the quality of the fit.

Parameter	This work	P. De Cat et al 2006 [25]
γ (km s^{-1})	−6.5335	
K (km s^{-1})	65.152	65.5(5)
e	0.0060289	0.0
ω (°)	215.922	
T_0	58268.4	
A sin*i* ($\times 10^6$ km)	1.1184	
Mass function	0.035772	0.0364(8)
P (days)	1.24843	1.24850

As seen above in table 3.10, the results obtained from the orbital fit carried out as part of this work agree with the results that have been previously published. This contrasts the agreements between the obtained parameters and previously published parameters, this could be attributed to this star not having any variations in the radial velocity measurements from stellar pulsations.

Table 3.11: Peak frequencies from FAMIAS analysis of spectroscopic observations of HD 85964.

	Frequency/d^{-1}	Relative Amplitude	S/N ratio
F_1	0.8008(1)	0.64(4)	32.806
F_2	1.6081(1)	0.04(4)	1.302
F_3	2.4041(1)	0.05(4)	1.183
F_4	3.2089(2)	0.06(4)	4.360

Presented above in table 3.11 are the results of the FAMIAS analysis of the 45 line profiles for HD 85964. Four pulsation frequencies were identified during this process all with a signal-noise ratio above 1.1 and a relative amplitude in the range of 0.40 to 0.64. As with the photometric analysis, these frequencies are all multiples of the binary orbital period so they cannot be attributed to stellar pulsations.

3.3.3 Comparison of Results

Table 3.12: Summary of calculated frequencies for HD 85964 calculated from both photometric and spectroscopic analysis.

$\text{Frequency}_P/d^{-1}$	$\text{Frequency}_S/d^{-1}$
0.8008(1)	0.8008(1)
1.60200(2)	1.6081(1)
2.4029(2)	2.4041(1)
3.2036(4)	3.2089(2)

As shown in table 3.12 above, the frequencies identified in both data sources do not agree within the error on the photometric frequencies apart from the lowest identified pulsation frequency. Discrepancies between the two sets of results emerge from the third decimal place onwards. This suggests that whilst the orbital fitting procedure is good, it still requires further improvement and modification to handle stars that exhibit any type of variability, whether that be stellar pulsations or elliptical.

3.4 Comparison of Results for All Stars

There are differences that can be seen in the frequencies obtained through photometric analysis and those that have been previously published, the difference in values obtained for HD 17310 are greater than the difference for values obtained for HD 217792. This could be attributed to there being more TESS observations of HD 217792 spread throughout the TESS mission whereas, HD 17310 only has two TESS sectors from the earlier phase of the mission. When more TESS observations have been taken this analysis could be repeated in order to determine whether the number of TESS observations has an effect on how accurate the results obtained by this method are and whether there are any discrepancies between the results published previously and those determined by this work.

More significant discrepancies in the results obtained within this work and previously published results begin to emerge from the fitting procedure used in order to obtain the binary orbital parameters. Within the fitting procedure used there is no accounting for variability in the measured radial velocities due to stellar pulsations, to further this work the fitting procedure used would need to be adapted in order to account for the variations in radial velocity that originate from stellar variability. This can be done by first averaging radial velocities with very small differences in order to determine the amplitude of any pulsations. More spectroscopic observations over longer time periods would also need to be taken as pulsations are not linked to orbital motion; by having a larger set of radial velocity measurements throughout the orbital cycle a truer picture of the orbital motion can be generated. By doing this, a more accurate set of orbital parameters can be obtained that are closer to the true orbital parameters; in turn this will better align the line profiles with the true nature of the pulsations and allow for more accurate pulsation frequencies to be identified from spectroscopic observations.

Agreement can be seen between the photometrically and spectroscopically determined frequency values to the first, and in most cases second, decimal place but most do not agree within the error of the photometric frequency. This suggests that, whilst there is some degree of consistency between the results, further work needs to be done in developing these techniques to ensure their accuracy. More light curves and an improved method of fitting the binary orbit will be required. The results from these improved techniques can be compared with those from both this work and previously published studies to highlight the improvements to techniques that are required in order to make accurate determinations of the pulsation frequencies for stars exiting in a binary star system.

By looking at a non-pulsator using the same methods as pulsators, discrepancies between the spectroscopically determined values can be attributed, in part, to the radial velocity fitting procedure. A greater difference between spectroscopically and photometrically determined frequencies can be seen for the pulsator stars. This has highlighted the need for further work and development of these methods in order to reduce such discrepancies in future works.

4. Conclusion

Pulsation frequencies were identified for three single-lined spectroscopic binary star systems, two of which were confirmed γ Dor pulsators and the other being an ellipsiodal variable, from both photometric and spectroscopic observations of the target stars. Periodograms were constructed using 120s cadence TESS light curves from which the pulsation frequencies of the stars were identified, aliases and combinations removed, and base frequencies determined. Line profiles taken from spectroscopic observations of the target stars were then used in order to determine the stars radial velocity at the time of observation using the moment method. These radial velocities were then used to construct a Radial Velocity curve for each of the target stars, this was then fitted using the StarSolve program (Milson, Barton & Bennet 2020) to obtain the stars orbital parameters. These orbital parameters were then used to calculate what the stars radial velocity should be at the times of observation assuming pulsations are occurring; the theoretical radial velocities were then subtracted from each of the line profiles in order to remove the effects of the Doppler shift caused by the binary motion of the star. The adjusted line profiles are then analysed using FAMIAS (W. Zima 2008), where a 1-D Fourier transform is constructed, frequencies are identified, and base frequencies determined in a similar manner as was done with the photometric results.

This work has shown that, whist existing analytical techniques provide good determinations of pulsation frequencies, further work is required in order to reduce the discrepancies seen between photometrically and spectroscopically determined pulsation frequencies. With the largest discrepancies being seen between the orbital parameters determined in this work and those from previously published studies, a good point to being further work in developing these techniques would be in improving the fitting procedures used for radial velocity curves to account for variations in radial velocity measurements due to stellar pulsation.

This work was intended to test existing asteroseismic analytical techniques and identify areas in which they can be improved upon for application to binary star systems. Many existing analytical procedures in asteroseismology do not account for binary motion and analytical procedures for binary stars do not account for variability being present from sources other than binary motion. Further work is required in both of these fields in order to develop analytical techniques that take account of variability originating from stellar pulsation and binary motion in order to obtained more accurate measurements of the pulsation frequencies of variable stars.

References

1. C. Aerts, “Probing the interior physics of stars through asteroseismology”, *Rev. Mod. Phys*. **93**,2021

2. S. Gill and P. F. L. Maxted et al, “The EBLM project VI. Mass and radius of five low-mass stars in F+M binaries discovered by the WASP survey”, *A&A*, **626**, A119, 2019

3. V. Niemela, “A Short History and Other Stories of Binary Stars, *RevMexAA (Serie de Conferencias)*, **11**, 23-26, 2001

4. T. Taurus and E. van den Heuvel, “Physics of Binary Star Evolution”, *Princeton University Press*, 2023

5. M. I. Swayne and P. F. L Maxted et al, “The EBLM project – VIII. First results for M-dwarf mass, radius, and effective temperature measurements using CHEOPS light curves”, *MNRAS*, **506**, 1, 306-322, 2021

6. P. F. L Maxted, A. H. M. J. Triaud and D. V. Martin, “The EBLM Project—From False Positives to Benchmark Stars and Circumbinary Exoplanets”, *Universe*, **9**, 12, 498, 2023

7. S. S. Shetye and G. Viviani et al, “VELOcities of CEpheids (VELOCE) II. Systematic Search for Spectroscopic Binary Cepheids”, arXiv:2405.19840v1 [astro-ph.SR] arXiv preprint arXiv:2405.19840. 2024

8. C. Aerts, J. Christensen-Dalsgaard, and D.W. Kurtz, “Asteroseismology”, *Springer Science & Business Media*, 2010

9. T. Padmanabhan. Theoretical Astrophysics: Volume 2, “Stars and Stellar Systems”, volume 2. *Cambridge University Press*, 2000.

10. G. Handler, “The Domain of Doradus Variables in the Hertzsprung-Russell Diagram.”, *MNRAS*, **309**(2):L19– L23, 1999.

11. R. Ouazzani, S.J.A.J. Salmon, and V. Antoci et al, “A New Asteroseismic Diagnostic for Internal Rotation in γ Doradus Stars.”, *MNRAS*, **465**(2):2294–2309, 2016.

12. A.C. Phillips, “The Physics of Stars.” Manchester Physics Series. *Wiley*, 1994.

13. W. Buscombe and P. M. Morris, “Three Southern Spectroscopic Binaries”, *MNRAS*, **123**, 2, 183–188, 1961

14. R. O. Gray and C. J. Corbally et al, “Contributions to the Nearby Stars (NStars) Project: Spectroscopy of Stars Earlier than M0 within 40 pc—The Southern Sample”, *AJ*, **132**, 161, 2006

15. P. R . Allen and A. J. Burgasser et al, “Low-mass Teriary Companions To Spectroscopic Binaries. I. Common Proper Motion Survey for Wide Companions Using 2Mass”, *AJ*, **144**, 2, 2012

16. D. Pourbaix, A. A. Tokovinin et al, “S_{B9}: The ninth catalogue of spectroscopic binary orbits”, *A&A*, **424**, 2, 727-732, 2004

17. H. A. Abt, “Observed Orbital Eccentricities”, *ApJ*, **629**, 507, 2005

18. V. Antoci and M. S. Bowman et al, “The first view of δ Scuti and γ Doradus stars with the TESS mission”, *MNRAS*, **490**, 3, 4040-4059, 2019

19. T. J. David and L. A. Hillenbrand, “THE AGES OF EARLY-TYPE STARS: STRÖMGREN PHOTOMETRIC METHODS CALIBRATED, VALIDATED, TESTED, AND APPLIED TO HOSTS AND PROSPECTIVE HOSTS OF DIRECTLY IMAGED EXOPLANETS”, *ApJ*, **804**, 146, 2015

20. A. Gáspár, G. H. Rieke, and N. Ballering, “THE CORRELATION BETWEEN METALLICITY AND DEBRIS DISK MASS”, *ApJ*, **826**, 171

21. L. E. Pasinetti Fracassini, L. Pastori, S. Covino and A. Pozzi. “Catalogue of Apparent Diameters and Absolute Radii of Stars (CADARS) - Third edition - Comments and statistics”, *A&A*, **367**, 2, 521-524, 2001

22. B. W. Bopp, D. S. Evans, J. D. Laing, T. J. Deeming, “Orbital Elements of Six Spectroscopic Binary Stars”, *MNRAS*, **147**, 4, 355-366, 1970

23. G. W. Henry, F. C. Fekel, and S. M. Henry, “Eleven New γ Doradus Stars, *AJ*, **129**, 6, 2005

24. R.F. Griffin, H.M.J. Boffin, “Spectroscopic Binary Orbits from Photoelectric Radial Velocities - Paper 191: HD 17310, HD 70645 and HD 80731”, *The Observatory*, **126**, 401-421, 2006

25. P. de Cat and L. Eyer et al, “A spectroscopic study of southern (candidate) γ Doradus stars - I. Time series analysis”, *A&A*, **449**, 1, 281-292, 2006

26. H. Bruntt, P. De Cat, and C. Aerts, “A spectroscopic study of southern (candidate) γ Doradus stars - II. Detailed abundance analysis and fundamental parameters”, *A&A*, **478**, 487–496, 2008

27. G. R. Ricker, J. N. Winn, “Transiting Exoplanet Survey Satellite”, *J. Astron. Telec. Instrum. Syst*, **1**, 0.14003, 2014

28. E. Brunsden and K. R. Pollard et al, “Spectroscopic pulsational frequency identification and mode determination of γ Doradus star HD 12901”, *Mon. Not. R. Astron. Soc.*, **427,** 2512–2522, 2012

29. J. M. Jenkins and J. D. Twicken et al, "The TESS science processing operations center," Proc. SPIE 9913, Software and Cyberinfrastructure for Astronomy IV, 99133E (8 August 2016);

30. Lightkurve Collaboration et al, 2018 ASCL

31. K. Bell, *AAS Meeting*, **235**, 106.06, 2020

32. J. B. Hearnshaw and S. I. Barnes et al, “The Hercules Échelle Spectrograph at Mt. John”, *Experimental Astronomy* ,**13**, 59–76, 2002

33. S. Pascual et al, “MEGARA Data Reduction Pipeline.”, *Highlights on Spanish Astrophysics X*, 227–227, 2019

34. N. Milson, C. Barton and P. D. Bennett, “A Python Code to Determine Orbital Parameters of Spectroscopic Binaries”, arXiv:2011.13914 **[astro-ph.SR]** https://doi.org/10.48550/arXiv.2011.13914

35. W. Zima, *Communications in Asteroseismology*, **155**, 2008